

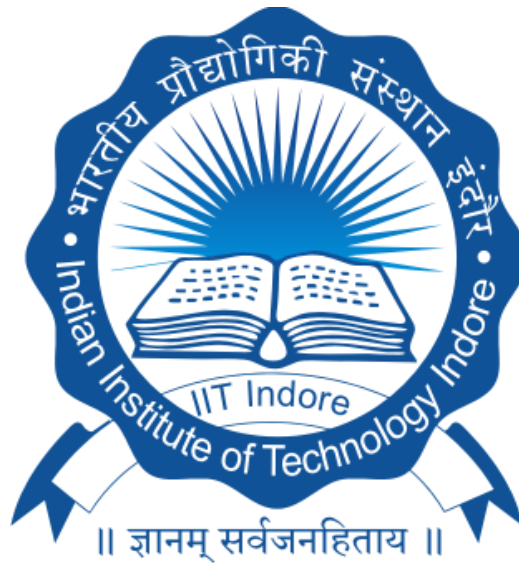
**Atomistic modelling of electromechanical response
of boron nitride nanotubes under buckling**

M.Tech. Thesis

By

Prakash Khatri

(1802103018)



**Discipline of Mechanical Engineering
Indian Institute of Technology Indore
JUNE 2020**

**Atomistic modelling of electromechanical response
of boron nitride nanotubes under buckling**

A THESIS

*Submitted in partial fulfillment of the
requirements for the award of the degree
of
Master of Technology*

by

**Prakash Khatri
(1802103018)**



**Discipline of Mechanical Engineering
Indian Institute of Technology Indore
JUNE 2020**

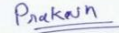


INDIAN INSTITUTE OF TECHNOLOGY
INDORE

CANDIDATE'S DECLARATION

I hereby certify that the work which is being presented in the thesis entitled **Atomistic modelling of electromechanical response of boron nitride nanotubes under buckling** in the partial fulfillment of the requirements for the award of the degree of **MASTER OF TECHNOLOGY** and submitted in the **DISCIPLINE OF MECHANICAL ENGINEERING, Indian Institute of Technology Indore**, is an authentic record of my own work carried out during the time period from July 2018 to May 2020 under the supervision of **Dr. Shailesh I. Kundalwal**, Discipline of Mechanical Engineering.

The matter presented in this thesis has not been submitted by me for the award of any other degree of this or any other institute.



Prakash Khatri
(1802103018)

This is to certify that the above statement made by the candidate is correct to the best of our knowledge.



Dr. Shailesh I.
Kundalwal

Prakash Khatri has successfully given his M.Tech. Oral Examination held on June 16, 2020.



Signature of the Thesis Supervisors
Date:



Signature of DPGC Convener,
Date:



Signature of the PSPC Member 1
Date:



Signature of the PSPC Member 2
Date:

Acknowledgment

First of all, I would like to express my gratitude to Dr. Shailesh I. Kundalwal for believing in me to carry out this work under their supervision. Their constructive support, friendly interactions, and constant encouragement have enabled this work to achieve its present form. Their innovative perspective towards things and continuous pursuit for perfection has had a profound effect on me and has transformed me majorly. I feel great To be one of his students.

I am thankful to Prof. Neelesh Kumar Jain, Director, IIT Indore, for allowing me to carry out the research work and providing all the facilities.

I am extremely thankful to Mr. Vijay Choyal for guiding me and helping me out from the very first day i joined this project. I would also like to express my thanks to all the members of the Atom Laboratory for their moral support and their friendly nature.

A heartfelt thanks to my entire M. Tech 2018-2020 Batch, with whom I have spent most of my time at IIT Indore.

Lastly, but undoubtedly the most valued, gratitude is expressed for my parents, for letting me choose my dreams and supporting me endlessly. Your unmatched support made this work possible.

PrakashKhatri

Dedicated to my Guide –

my mother,

my father,

my sister,

my brother,

my teacher,

and my friends

Abstract

Buckling is the major failure modes of boron nitride nanotube, piezoelectricity in nanotubes significantly affected by an electric field. In this work, boron nitride nanotube (BNNTs) is taken as an example to investigate issues based on molecular dynamics simulation. Three-body Tersoff potential force field is used to see buckling effect and piezoelectric response of BNNTs. Furthermore, to formulate the piezoelectric coefficient of boron nitride nanotubes, an integrated computational method is used in this method for formulation of mathematical relationship. Genetic programming and molecular dynamics simulation is used for the piezoelectric coefficient of BNNTs. The results show that critical buckling is majorly affected by the electric field. In zigzag BNNTs, increase in electric field buckling strain decreases and for armchair BNNTs, increase in the electric field no significant change in buckling strain. For (0, 17) zigzag BNNTs, piezoelectric coefficient 0.3125 C/m^2 is reported. Our results reveal that the vacancy defect significantly influences the buckling stress and piezoelectric properties. By generating 1% random vacancies in BNNTs, the buckling stress reduces to 59%, buckling strain reduces to 35%, and the piezoelectricity coefficient reduces to 11%. For Stone-Wales defect, buckling stress decreases but a change in piezoelectric coefficient is not significant. The results show that buckling can be controlled by applying the electric field.

Contents

| | |
|---|----------------------------|
| Acknowledgment..... | 4 |
| Abstract..... | 6 |
| List of Publications..... | 9 |
| List of Figures | 10 |
| List of Table..... | 12 |
| Chapter 1 | Introduction 13 |
| 1.1 Nanotechnology | 13 |
| 1.2 Nanotubes | 13 |
| 1.3 Nanomechanics | 14 |
| 1.4 Boron Nitride Nanotubes..... | 15 |
| 1.5 Classification of Boron nitride nanotubes | 15 |
| 1.5.1 Single wall boron nitride nanotubes | 15 |
| 1.5.2 Multi-wall boron nitride nanotubes (MBNNTs) | 16 |
| 1.6 Chirality..... | 17 |
| 1.7 Defects..... | 18 |
| 1.8 Types of defects in BNNTs | 19 |
| 1.8.1 Vacancy defects (Point defects) | 19 |
| 1.8.2 Stone-Wales defects (Topological defects)..... | 20 |
| 1.9 BNNTs Applications..... | 20 |
| 1.10 Synthesis Methods of Boron Nitride Nanotubes | 21 |
| 1.10.1 Arc-Discharge Methods | 21 |
| 1.10.2 Laser Ablation Method | 22 |
| 1.10.3 Ball Milling & Annealing Method | 22 |
| Chapter 2 | Literature review 23 |

| | |
|--|-----------------------------|
| 2.2 Motivation | 26 |
| 2.3 Research objectives | 26 |
| Chapter 3 | Methodology |
| | 27 |
| 3.1 Computational Methods | 27 |
| 3.2 Molecular Dynamics Simulation | 27 |
| 3.4 Integration Algorithms | 28 |
| 3.4.1 The Velocity Verlet Algorithm | 28 |
| 3.5 Statistical Ensembles | 29 |
| 3.5.1 Micro-canonical Ensemble (NVE) | 30 |
| 3.5.2 Canonical Ensemble (NVT) | 30 |
| 3.5.3 Isothermal-Isobaric (NPT) Ensemble | 30 |
| 3.6 Potential Fields..... | 31 |
| 3.7 Flowchart for MD simulations..... | 33 |
| 3.8 Atomistic modeling of BNNTs..... | 33 |
| 3.9 Genetic programming model | 38 |
| Chapter 4 | Results and discussion..... |
| | 41 |
| 4.1 Effect of vacancy defect | 45 |
| 4.2 Stone-wales defect effect..... | 48 |
| 4.3 Genetic programming..... | 51 |
| 4.4 Conclusion: | 54 |
| Reference | 55 |

List of Publications

1.”Buckling and piezoelectric response of boron nitride nanotubes under electric field: A MD study”.VijayChoyal, PrakashKhatri and S. I. Kundalwal*

2. “ Effect of electric field on buckling analysis of boron nitride Nanotubes.”(COPEN 2019), IIT Indore, Vijay Choyal, PrakashKhatri, V. K. Choyal, and S. I. Kundalwal*

List of Figures

| | |
|---|----|
| Figure 1 A boron nitride nanotube model..... | 13 |
| Figure 2: Nanomechanical model | 14 |
| Figure 3: Single-wall boron nitride nanotube | 16 |
| Figure 4: Multi-wall boron nitride nanotube. | 17 |
| Figure 5: Representation of chirality in sheet and nanotube..... | 18 |
| Figure 6: Vacancy defect concentration | 19 |
| Figure 7: Stone-wales defect..... | 20 |
| Figure 8: Arc discharge method..... | 22 |
| Figure 9: Graphical representation of MD process | 27 |
| Figure 10: Change in position of an atom with respect to time | 29 |
| Figure 11: Graphical representation of the different ensembles | 31 |
| Figure 12: Change in positions and velocities of atoms with time | 31 |
| Figure 13: Force field degree of freedom | 32 |
| Figure 14: Flow chart of molecular dynamics simulation | 33 |
| Figure 15: Different concentration vacancy defect | 37 |
| Figure 16: Schematic representation of applied electric field on (a) armchair and (b) zigzag BNNTs | 38 |
| Figure 17: Subtree crossover operation | 40 |
| Figure 18: Subtree mutation operation | 40 |
| Figure 19: Axial compressive stress-strain curve for BNNTs | 41 |
| Figure 20: Structures of BNNTs under compression from points A to C. | 42 |
| Figure 21: Stress-strain curve of zigzag (0, 17) BNNTs subjected to the different electric field. | 42 |
| Figure 22: Stress-strain curve of Armchair (10, 10) BNNTs subjected to the different electric field..... | 43 |
| Figure 23: Variation of stresses in pristine (0, 17) BNNTs with the Electric field..... | 44 |
| Figure 24: Schematic representation of vacancy concentration of 0%, 1% and 2% for zigzag (0, 17) BNNTs..... | 45 |
| Figure 25: The stress-strain curve with vacancy defect zigzag BNNTs.... | 46 |

| | |
|---|----|
| Figure 26: Stress-electric field curve vacancy defected zigzag BNNTs. ... | 47 |
| Figure 27: Schematic representation of stone wales defects by rotating B–N bonds 0, 1, and 2 for zigzag (0, 17) BNNTs. | 48 |
| Figure 28: The stress-strain curve with stone-wales defect zigzag BNNTs. | 49 |
| Figure 29: The snapshot of failure process in BNNTs under axial compression loading of zigzag (0, 17) BNNT. | 50 |
| Figure 30: The snapshot of the failure process of stone wales defected BNNTs under axial compression loading of zigzag (0, 17) BNNT. | 50 |
| Figure 31: The snapshot of the failure process of vacancy defected BNNTs under axial compression loading of zigzag (0, 17) BNNT. | 51 |

List of Table

| | |
|---|----|
| Table. 1 Buckling stress and buckling strain of different vacancy defected BNNTs..... | 45 |
| Table.2 Buckling stress and buckling strain of different stone wales defected BNNTs..... | 48 |
| Table 3: Descriptive statistics of the input and output process variables obtained from MD simulations for BNNTs..... | 52 |
| Table 4: Parameter settings for the proposed MD based AI model..... | 53 |

Chapter 1 Introduction

1.1 Nanotechnology

Nanotechnology is the study of matter on a molecular and atomic level. It is usually supposed to deal with devices, material, and other structures in the size range of less than 100 nm. This is a distinct field of completely new approaches, extending from traditional instrument physics based on molecular self-assembly. Testing new materials with dimensions at the nanoscale to see if we can directly control matter at the atomic level. The main field of nanotechnology involves researchers from many different disciplines, including biologists, chemistry, physicists, and engineering. Various research work and development is going on in the field fo cancer detection and treatment[1].

1.2 Nanotubes

The formation of the nanotube is done by rolling a 2-D sheet into a cylindrical form of particular atoms. The size of nanotubes is in nanometers to 100 micrometers. Different material based nanotube making possible by material like carbon- and boron-nitrogen. distinctive properties of this nanotubes attract researchers' attention to recent years. Figure 1 showsanexample of the boron-nitride nanotube.

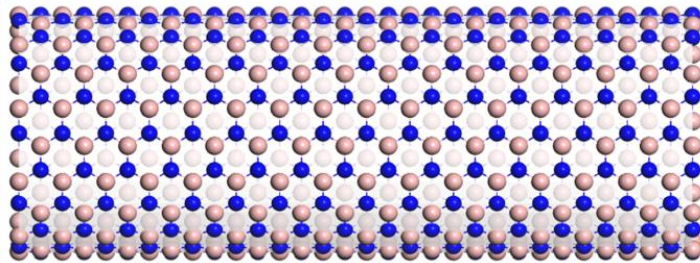


Figure 1 A boron nitride nanotube model

Nanotubes are very toughest in nature. They have varies distinctive properties like high thermal resistance, mechanical strong, stable, and

electromechanical properties, and these properties depend on which nanotube you have taken.

1.3 Nanomechanics

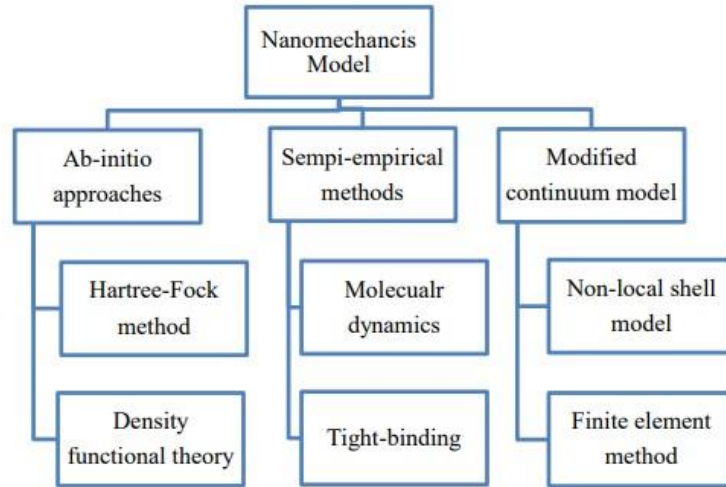


Figure 2: Nanomechanical model

At nanoscale fundamental studies like thermal, kinetic, and elastic properties were studied by using nanomechanics. For structure if any one dimension is less than 100 nm is called a nanostructure. Current experimental studies at the nanometer scale are very costly also take a very long time to execute the experiments that why theoretical studies play a very important role in nanotechnology. We can subdivide models of nanomechanics which are ab-initio, semiempirical, and modified continuum models shown in Figure 2. The first principle which is also called ab-initio methods such as density function theory [2] and Hartree-Fock [3] method usually gives more accurate results reason for this because the ab-initio starts with basic equation for the whole system. Ab-initio method is not suitable for large nanostructure systems such as boron nitride sheets or carbon sheets. Molecular dynamics comes under the semi-empirical method. This approach is taking less time also done in

very less cost as compare to the ab-initio approach and give competitive results. In the semi-empirical method molecular dynamics is the most popular approach in this interaction between molecules is define by using molecular level force fields.

1.4 Boron Nitride Nanotubes

The Boron nitride nanotubes (BNNTs) grab the researcher's attention after discovered in 1994 [4]. Boron nitride and carbon-based nanostructure have similar lattice structures and BNNTs can be created by rolling of two-dimensional boron nitride nanosheets (h-BNNs).

The BNNTs have large bandgap (5.60eV), thermally and chemically more stable, good piezoelectric and flexoelectric properties, and greater hardness than the carbon-based counterpart [5][6]. Also, thermal oxidation resistance is greater in BNNTs as compare to carbon nanotubes (CNTs) which make BNNTs more suitable for aerospace activities. Furthermore, BNNTs are stable up to 850°C in the normal atmosphere [7] in the dissimilarity of CNTs starts to oxidize at 300°C under similar conditions. BNNTs have excellent radiation shielding properties. Also, BNNTs are proven to be the best applicants for emphasizing metal-ceramic, and matrix composite, which is usually manufactured at high temperatures [5]. Outstanding properties of BNNTs make it more suitable for many multifunctional applications like hydrogen storage [8][9], optoelectronics and transistors, and composite material [10].

1.5 Classification of Boron nitride nanotubes

1.5.1 Single wall boron nitride nanotubes

single wall boron nitride nanotube is formed by a single sheet of boron and nitrogen, its diameter dimension is close to 1 nm, and the length dimension is various from 10 nanometers to 100 micrometers [10]. rolling of BN sheet is depend on indices vector (n, m). n and m are miller indices

a number of unit vectors along two-directional in the hexagonal crystal lattice in boron nitride sheet. according to n and m, three types of the nanotube is possible zigzag, armchair, and chiral nanotube

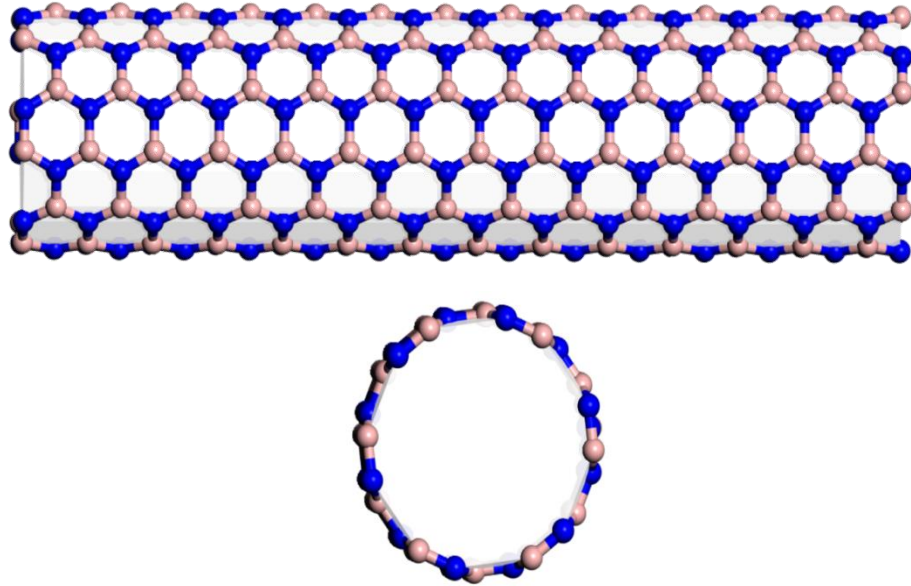


Figure 3: Single-wall boron nitride nanotube

1.5.2 Multi-wall boron nitride nanotubes (MBNNTs)

Multi-wall boron nitride nanotube (MWBNNNT) formed by rolling multiple boron nitride sheets. The distance between two nanotubes which is called interlayer distance in multi-wall boron nitride nanotube is 3.34 \AA [11]. Due to relative diameter limitation and geometry probability of the singular tube, The whole multi-wall nanotube has a zero-gap metal. there properties and morphology are similar to single wall nanotube but MWBNNT shows very good resistance to chemicals which will add up more properties in boron nitride nanotubes.

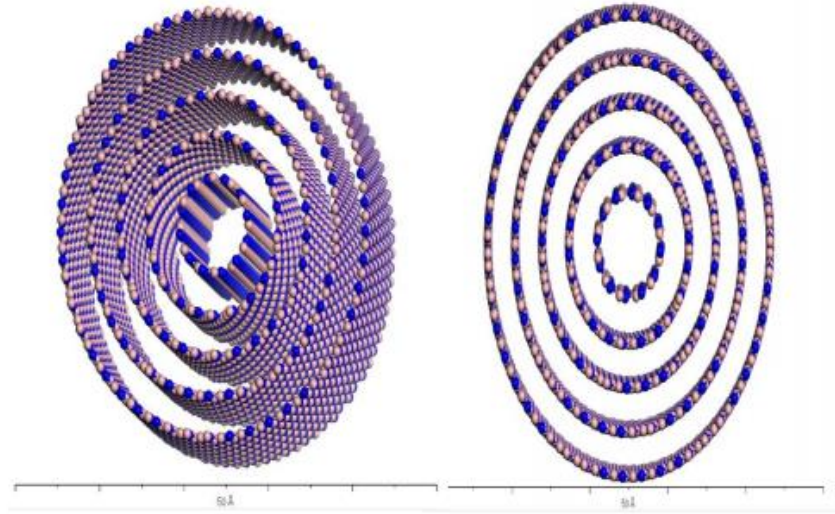


Figure 4: Multi-wall boron nitride nanotube.

1.6 Chirality

Chirality is used for defining the geometry and type of structure using chirality. It has been found that three types of nanotube which are zigzag, armchair, and chiral boron nitride nanotube. Here we only studied the zigzag and armchair nanotube. The rapping of the boron nitride sheet is done by using chiral indices (n, m) where n and m are chiral roll-up vector [12]. Figure 5 shows the chiral vectors [13]. Chiral vector C_h can be represented as follows:

$$C_h = n\mathbf{a}_1 + m\mathbf{a}_2 \quad (1)$$

Where \mathbf{a}_1 and \mathbf{a}_2 are the unit vector in the boron nitride sheet and n, m are miller indices.

Using Miller indices we can calculate the diameter of the nanotube as follows

$$d = \frac{a_0}{\pi} \sqrt{(n^2 + m^2 + mn)} \quad (2)$$

Where $a_0 = 1.446 \text{ \AA}$ (Bond length)

We can define the type of nanotube by Miller indices n, m as follows if n and m are equal than nanotube is called armchair nanotube and chiral angle is 30° , if m is equal to zero value than nanotube is called zigzag nanotube with a chiral angle equal to 0° , and if m is not equal to zero than nanotube is called chiral nanotube with chiral angle value lie between 0° and 30° .

To see the structure of the different types of BNNT Figure 5 shows the BN sheet and nanotube of zigzag and armchair chirality[12].

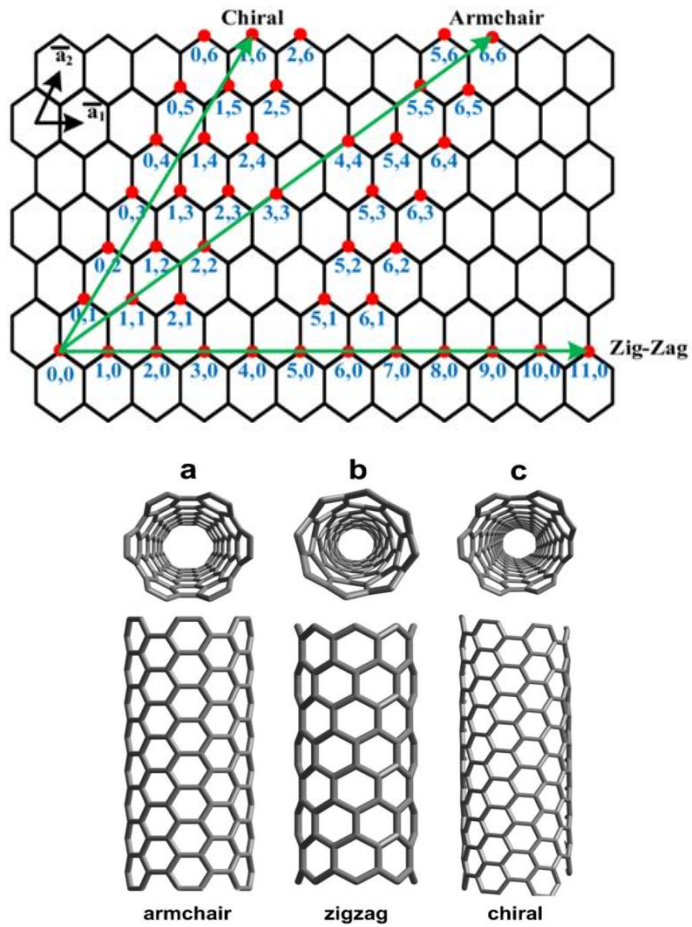


Figure 5: Representation of chirality in sheet and nanotube

1.7 Defects

Defects in nanotube play a very important role in defining the material properties of nanotube. rearrangement of molecules or absent of molecules from there position causes the defects in nanotube [14]. if defects are

present in nanotube these defects weaker the structure which causes a reduction in buckling and tensile strength. various defects present in nanotube are dislocation defect, vacancy defect, and Stone-wales defect these defects present in nanotube reduce the thermal, electronic, and mechanical properties [14].

1.8 Types of defects in BNNTs

Various types of defects present in BNNTs describe below

1.8.1 Vacancy defects (Point defects)

From pristine BNNTs, if boron or nitrogen atom is not present in there position [15]. this type of defect is called vacancy defect. These defects are introducing in BNNTs during the manufacturing process these defects alter the properties of BNNTs. vacancy defects reduce the mechanical, electrical, and thermal properties of BNNTs [16]. Figure 6 shows the vacancy defected nanotube. In the present work randomly generated vacancy is considered in vacancy concentration form. in the computational model, we can generate the defects. the vacancy concentration percentage is calculated using the following formula

$$\rho = \frac{\text{sum of removed atoms}}{\text{sum of all atom in BNNTs before defect}} \times 100 \quad (3)$$

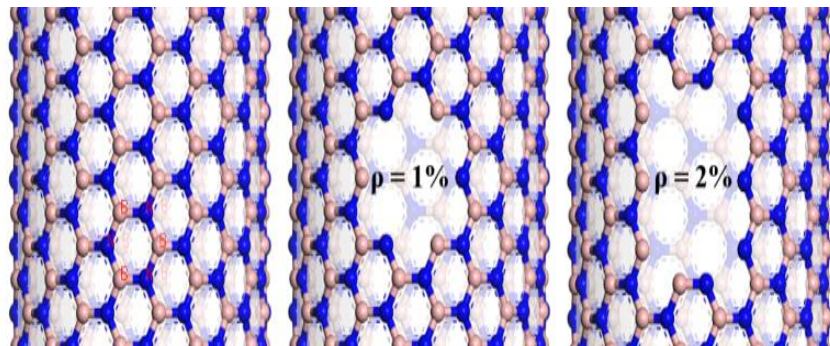


Figure 6: Vacancy defect concentration

1.8.2 Stone-Wales defects (Topological defects)

First of all stone-wales defect is investigated by Song et al [17]. Experimental results and simulations are shown to show the stone-wales defect. In this defect, two pi bonds rotate 90° from their midpoint of the bond, and it will convert two hexa- structures to one penta- and one hepta- structure in nanotube [17]. This is called stone-wales transformation, this defect generates two unfavorable homoelement which is B-B and N-N. This defect affects the mechanical and electrical properties of the BNNTs. The figure shows the stone-wales defect.

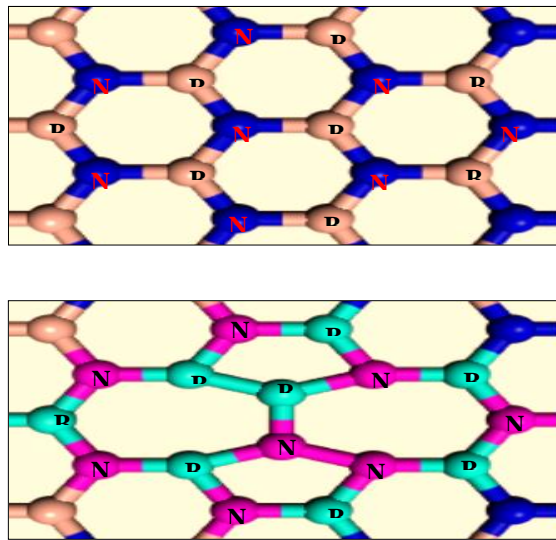


Figure 7: Stone-wales defect

1.9 BNNTs Applications

The Boron nitride nanotubes (BNNTs) grab researchers' attention after discovered in 1994. Boron nitride and carbon-based nanostructure have similar lattice structures and BNNTs can be created by rolling of two-dimensional boron nitride nanosheets (h-BNNs). The BNNTs have large bandgap, thermally and chemically more stable, good piezoelectric and flexoelectric properties, and greater hardness than the carbon-based counterpart. Also, thermal oxidation resistance [18] is greater in BNNTs as compare to carbon nanotubes (CNTs) which make BNNTs more

suitable for aerospace activities.. Furthermore, BNNTs are stable up to 850°C in the normal atmosphere in the dissimilarity of CNTs start to oxidize at 300°C under similar conditions. BNNTs have excellent radiation shielding properties. Also, BNNTs are proven to be the best applicants for emphasizing metal-ceramic, and matrix composite, which is usually manufactured at high temperatures. Outstanding properties of BNNTs make it more suitable for many multifunctional applications like hydrogen storage, optoelectronics and transistors, and composite material.

1.10 Synthesis Methods of Boron Nitride Nanotubes

There are various methods used for synthesis boron nitride nanotubes few of them are discussed below.

1.10.1 Arc-Discharge Methods

The first technique for synthesis for carbon as well as boron nitride nanotubes is the arc discharge method. In this method, for arc-discharge reactants are used, and electrodes are applied between these electrodes. Figure 8 shows the schematic representation of this method. 500 Torr pressure is maintained inside the chamber and 20-40 V and 150 A current maintained for performing this method. the gap between the two electrodes is maintained low as 1mm. during this method, the temperature reaches upto 4000K. consumption of electrode is done by anode reason for this is electron from the arc-discharge is accelerated and strike towards the anode. deposition of nanotubes are done at the cathode.

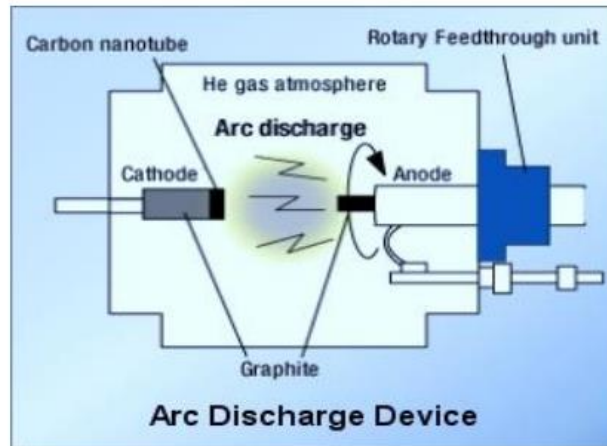


Figure 8: Arc discharge method

1.10.2 Laser Ablation Method

In this method, a continuous beam is sent to target (for boron nitride nanotube target is a source of boron) this set up is present inside a furnace. thereaction of boron is happening with nitrogen source gas. In vary,theshort-time temperature reaches to few hundreds of Kalvin by laser. from the furnace a carrier gas is passed during laser ablation. this carried gas collect the nanotube on the cold metal trap[19].

1.10.3 Ball Milling & Annealing Method

This method complete in a two-step. first of all, at room temperature, a ball milling is carried out, and then annealing is performed. A stainless steel cell is used to load the source of boron. there are several steel balls inside the cell. gas like NH_3 or N_2 is filled inside the milling chamber which actsasasource of nitrogen. then this chamber starts to rotate and balls start to collide with boron source powder. after performing the first step we go for the second step in which boron powder is put into a furnace and anneal with nitrogen source gas up to 10000C. this method is used for synthesis large quantity at low cost.

Chapter 2 Literature review

BNNTs show his outstanding properties that's attracts a lot of researchers who have been working on the synthesis and perform a computational study of MWBNNTs.

Recent years of extraordinary properties of nanotube attract lots of researchers' attention. The superior study of carbon nanotubes (CNTs) by Iijima[20]and their electrical[21],thermal[20], [22]–[25], and mechanical [20], [23]–[25]properties were encouraged the other type of nanotube.Boron nitride nanotube shows more distinct properties.

Numerous researchers are doing work to find mechanical and electrical properties by both experimental techniques and computational methods.Axial compression and buckling behaviour of CNTs was studied.Liew et al. [26] studied that increasing the diameter of nanotube results in an increase in buckling load. Kang et al. [27]studied the carbon nanotube subjected to compression nanotube-based intermolecular junction using finite element analysis and molecular dynamics (MD) simulation. Yan et al. [28] studied the buckling of multi-wall CNTs under temperature field using nonlocal elastic shell theory and there study shows that the critical compression load is shown inverse relation with temperature. Liew and Yuan [29] studied the structural performance using the computational modeling approach at high temperature and compression of double-wall BNNT and their results show that thermal stability and compressive strength of BNNTs are superior to CNTs. Shokuhfar et al. [30] used MD simulation to study the buckling strength of BNNTs at different temperatures. They found that at higher temperature buckling strength decreases. Furthermore, with increasing the length of BNNTs the buckling resistance decreases. Ebrahimi-Nejad and Shokufar[31]. studied the buckling strength of BNNTs for hydrogen storage. The literature review discussed above shows that buckling strength is depend mainly on chirality, various defects, temperature, and

system size. Therefore for the effective study of piezoelectric properties, we need to consider all these points in our work.

Khojin et al. [32] studied the buckling and electro-thermomechanical loading of BNNTs reinforced piezoelectric polymeric composite and they found that buckling resistance enhanced by piezoelectric matrix, and the elastic medium is depending on the direction in which electric field is applied. Jafari et al. [33] studied the mechanical and electrical properties of nanostructures using a continuum mechanics approach. Zhang et al. [34] studied the effect of electric field on the buckling and fracture of the GaN nanowires and their study shows that as we increase the electric field the critical buckling strain decrease and tensile strain increases. Yamakov et al. [35] used MD simulations to investigate the piezoelectric of BNNTs subjected to twist and tensile forces and they found that polarization of BNNTs depends on their geometrical configurations. Yamakov et al. [36] investigate the multi-walled BNNTs piezoelectric and elastic response using a classical MD simulation and their study shows that electromechanical properties depend on the diameter of BNNTs. And they also found that change size significantly affects the piezoelectric properties especially polarization decreases as we increase the diameter of BNNTs. It is also reported that the zigzag BNNTs show higher axial piezoelectric coefficients than the armchair tubes [37][38].

BNNTs are being synthesized by using various techniques such as laser ablation [39], arc discharge [40] these manufacturing processes promote the presence of different topological defects such as antisites, Thrown-Stone-Wales (TSW) [17], doping [15], vacancies due to inherent limitation of the fabrication and purification processes. Apart from mechanical properties these defects also influence the electronic properties of BNNTs. Song et al. [17] study the effect of Stone-Wales defect of BNNTs using atomistic/continuum model. Li et al. [41] investigate how the electronic structure of BNNTs and their nanocomposites affect by the

topological defects. Griebel et al. [42] investigated the BNNTs using Tersoff potential and see the effect of vacancies using molecular dynamics simulations and their study shows that elastic modulus of BNNTs significantly decreases as we increase the vacancy defects. Paura et al. [43] studied the vacancy defect of BNNTs and found that electronic structure of BNNTs is strongly influenced by vacancy defects. Wang et al. [44] investigate the strength, failure, and stiffness of BNNTs containing vacancy and Stone-Wales defects using DFT. They found that vacancy defect shows a more change in the mechanical properties as compared to Stone-Wales defects under axial deformation. Choyal et al. [45] studied the effect of vacancy defect on the electronic and elastic properties of transversely isotropic BNNTs using MD simulation. They found that as vacancy concentration increases the transversely isotropic elastic constant of BNNTs decreases. Zeighampour et al. [46] investigate the buckling analysis with the defect and without defected BNNTs using MD simulation their study shows that as we increase the defect buckling decreases.

The literature review indicated that lots of studies carried out for buckling and piezoelectric response of BNNTs. To the best of the current author's knowledge, there is no single study exists which shows buckling analysis of BNNTs under electric field effect and piezoelectric response. Also see the effect on vacancy and Stone-Wales defect in BNNTs mechanical and piezoelectric properties. Also, stabilized the relationship for length and vacancy defect with the piezoelectric coefficient using genetic programming.

2.2 Motivation

molecular dynamics are widely used for computational work because of less time consuming and cost-effectiveness. boron nitride nanotubes have a wide range of thermal, mechanical, and electrical properties also BNNTs have a large bandgap and it shows excellent piezoelectric properties. during the manufacturing process, different types of defects occur in nanotubes like a topological defect, vacancy defect, stone-wales defects, etc. the influence of these defects is very large in properties of BNNTs. the electric field also affects the mechanical strength of BNNTs.

2.3 Research objectives

- Computational study of Piezoelectric response of zigzag and armchair BNNTs, to develop a computational model for predicting critical buckling stress of BNNTs.
- To investigate the electric field effect on buckling Finding piezoelectric response of BNNTs subjected to the electric field and compressive strain.
- Determine the critical stress, piezoelectric response, and see effects of vacancy and stone-wales defected BNNTs via MDS.
- Integrated MD based AI simulation technique (Genetic Algorithm) for formulating the relation using data obtained from MD simulation

Chapter 3 Methodology

3.1 Computational Methods

computational simulation is the method to study the mathematical model it is a modern tool for numerical study and sees complex system behaviour by this mathematic model in the form of computer simulation. Molecular dynamics is a widely used computational method, this method is cost-effective also takes a small time in simulation as compared to others. In molecular dynamics it computes the motion of every molecule, and uses Newton's law of motions, which gives momentum and position of molecules. By using molecular dynamics we can simulate the system in every environment without any experiments which save our time and cost [47].

3.2 Molecular Dynamics Simulation

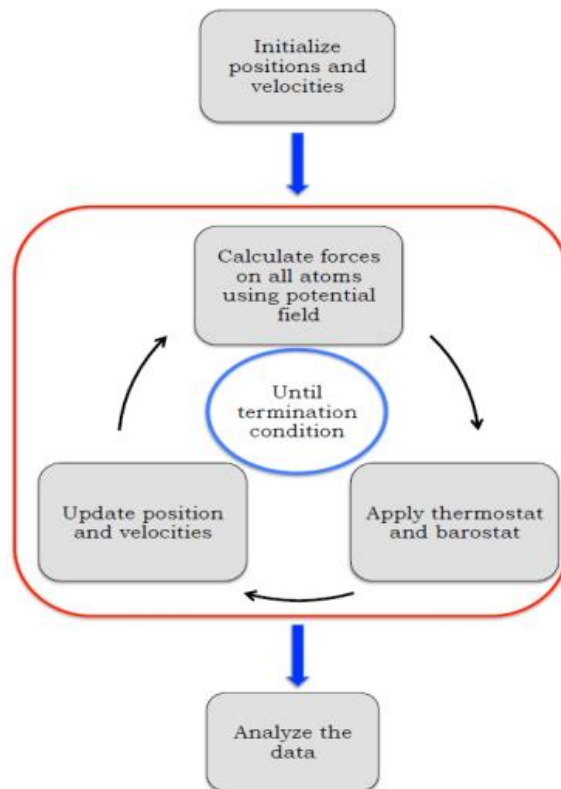


Figure 9: Graphical representation of MD process

Molecular dynamics is a simulation method in which we analyze the movement of molecules and atom. this is achieved by integrating their equation of motion. and integration is achieved by solving newton's equation of motion. the potential force field is used to define the interaction between two atoms. Molecular dynamics is less time consuming and cost-effective method. Also, we can generate a natural environment in molecular dynamics by thermodynamics ensembles in present work we use LAMMPS (large-scale atomic/molecular massively parallel simulator) which is open-source software.

3.4 Integration Algorithms

Integration algorithm is used for finding initial value problem in molecular dynamics simulation we have a position of atoms, potential energy is the function of this position. these functions are very complex [48]. this equation is solved numerically. various integration method is available but velocity verlet algorithm is an efficient method in our study we use velocity verlet algorithm. a suitable environment for velocity verlet algorithm is it requires one energy evaluation, it should be fast, small computer memory allocation requires, require low time step, shows conservation of energy.

3.4.1 The Velocity Verlet Algorithm

integration of newton's equation of motion is done by using velocity verlet algorithm. in one-time step, atoms are allowed to move and accelerate. The new position of an atom is obtaining by using this acceleration data and integration of motion equation which is velocity verlet algorithm. below shows the velocity verlet algorithm.

$$\mathbf{V}\left(t_o + \frac{\Delta t}{2}\right) = \mathbf{V}(t_o) + \mathbf{a}(t_o) \frac{\Delta t}{2} \quad (4)$$

$$\mathbf{r}\left(t_o + \frac{\Delta t}{2}\right) = \mathbf{r}(t_o) + \mathbf{V}\left(t_o + \frac{\Delta t}{2}\right) \Delta t \quad (5)$$

$$V\left(t_0 + \frac{\Delta t}{2}\right) = V\left(t_0 + \frac{\Delta t}{2}\right) + a(t_0)\Delta t \quad (6)$$

Where,

r = position of the atom,

V = Velocity of the atom,

a = acceleration of the atom.

T_0 = initial time,

Δt = time step,

Variation of position, velocity and time step is shown in figure

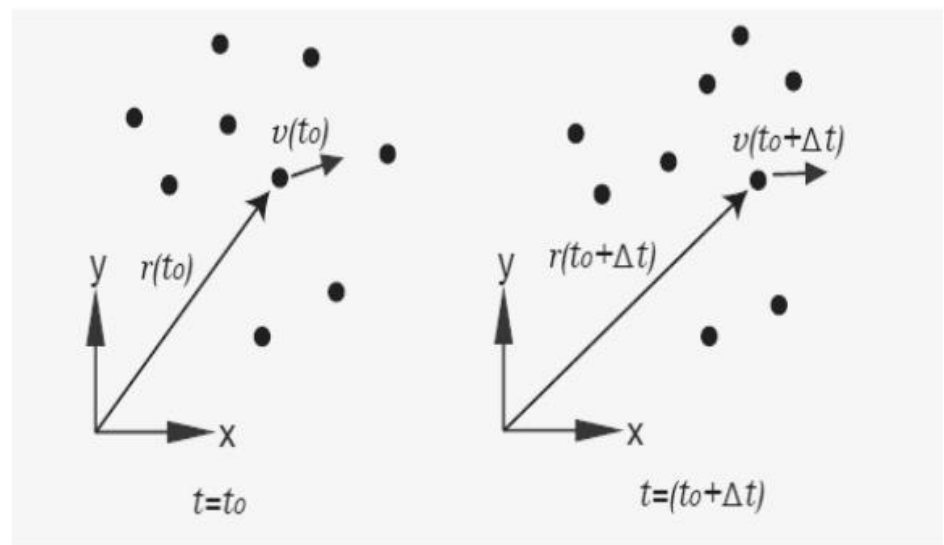


Figure 10: Change in position of an atom with respect to time

Creating a natural environment in simulation control of pressure and temperature is necessary for the system. molecular dynamics simulations are carried out in constant pressure and constant temperature this is achieved by controlling there velocity and size of the simulation box. controlling of these properties is discussed below.

3.5 Statistical Ensembles

The constant energy surface of the system is studied by integrating newton's equation of motion. various natural system process occurs under different pressure and temperature condition system transfer heat to the environment or absorbs heat from environment therefore total energy of

the system is not conserved that's for simulation purpose we need thermodynamics condition for maintaining a natural environment which is discussed below.

3.5.1 Micro-canonical Ensemble (NVE)

NVE is a thermodynamic ensemble in which the number of atoms of system, volume of the system, and energy of the system remain constant [49]. this is obtained by solving newton's equation of motion. this is an adiabatic ensemble therefor energy is conserved during the process but there is a possibility of some truncation and rounding error.

3.5.2 Canonical Ensemble (NVT)

NVT is a thermodynamic ensemble in which the number of atoms of system, volume of the system, and Temperature of the system remain constant [49]. this is also called conical ensemble and some time referred to as constant temperature molecular dynamics simulation. In this method energy of the exothermic and endothermic process is exchange. This is suitable when we carried out our simulation is without boundary condition and in a vacuum.

3.5.3 Isothermal-Isobaric (NPT) Ensemble

NVT is a thermodynamic ensemble in which the number of atoms of system, pressure of the system, and Temperature of the system remain constant [49]. the pressure is changed by a change in volume and temperature is maintained constant by a change in velocity of atoms. this method is taken when correct volume, density, and pressure are important in simulation. this ensemble mainly used in the equilibrium process for achieving stable conditions.

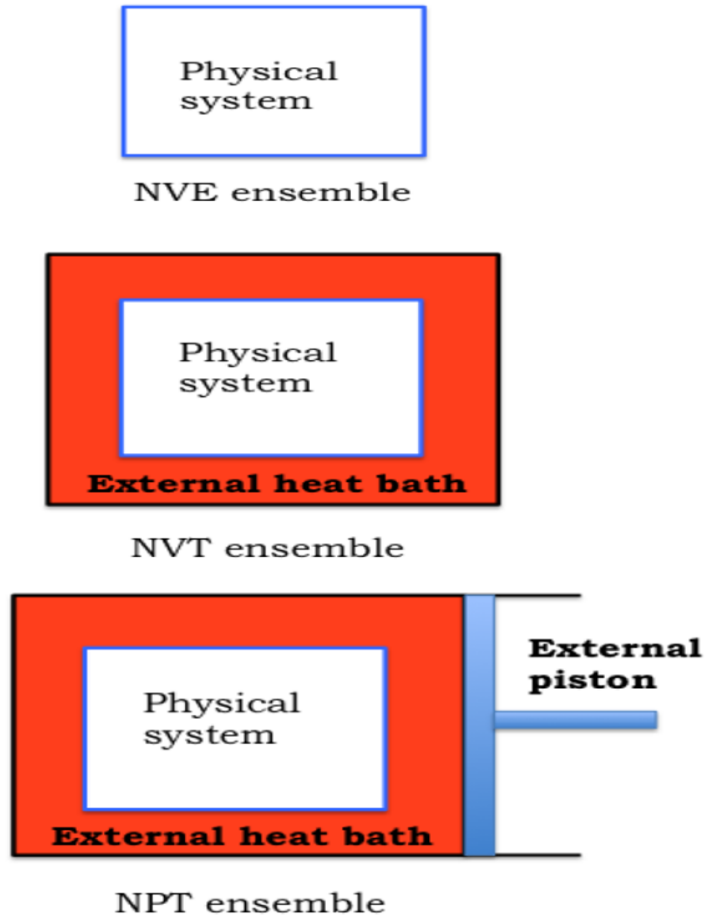


Figure 11: Graphical representation of the different ensembles

3.6 Potential Fields

For any computational method potential field play a very important role in simulation, this potential field is the mathematical expression of the potential energy of atoms [50]. The parameters of potential fields mainly obtain from experimental methods. in our work, we use three body tersoff potential. we can express the potential field as

$$E_{total} = E_{covalent} + E_{non\ covalent} \quad (7)$$

Where,

E_{total} = total energy

$E_{covalent}$ = covalent energy

$E_{\text{non-covalent}}$ = non-covalent energy

We can further express no-covalent and covalent energy as,

$$E_{\text{covalent}} = E_{\text{bond}} + E_{\text{angle}} + E_{\text{dihedral}} + E_{\text{out-of-plane}} \quad (8)$$

$$E_{\text{non covalent}} = E_{\text{electrostatic}} + E_{\text{vander Waals}} \quad (9)$$

The Lennard Jones interactions or van der Waal's interactions are given by

$$E_{ij} = 4\epsilon_{ij} \left[\left(\frac{\sigma_{ij}}{r_{ij}} \right)^{12} - \left(\frac{\sigma_{ij}}{r_{ij}} \right)^6 \right] \quad (10)$$

Here σ is called equilibrium spacing parameter of the Lennard-Jones potential and it was obtained as the arithmetic mean of the individual parameters of the respective atom. and the geometric mean of the value of the respective atom types is called depth parameter ϵ . distance between two non bonding atom is r .

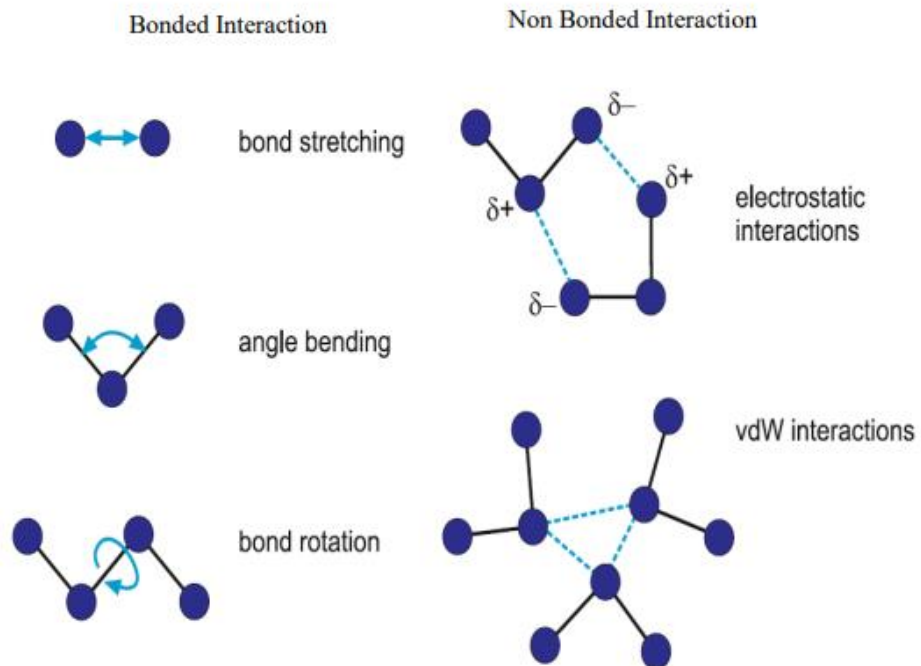


Figure 13: Force field degree of freedom

3.7 Flowchart for MD simulations

The figure is shown the MD simulation flow chart,

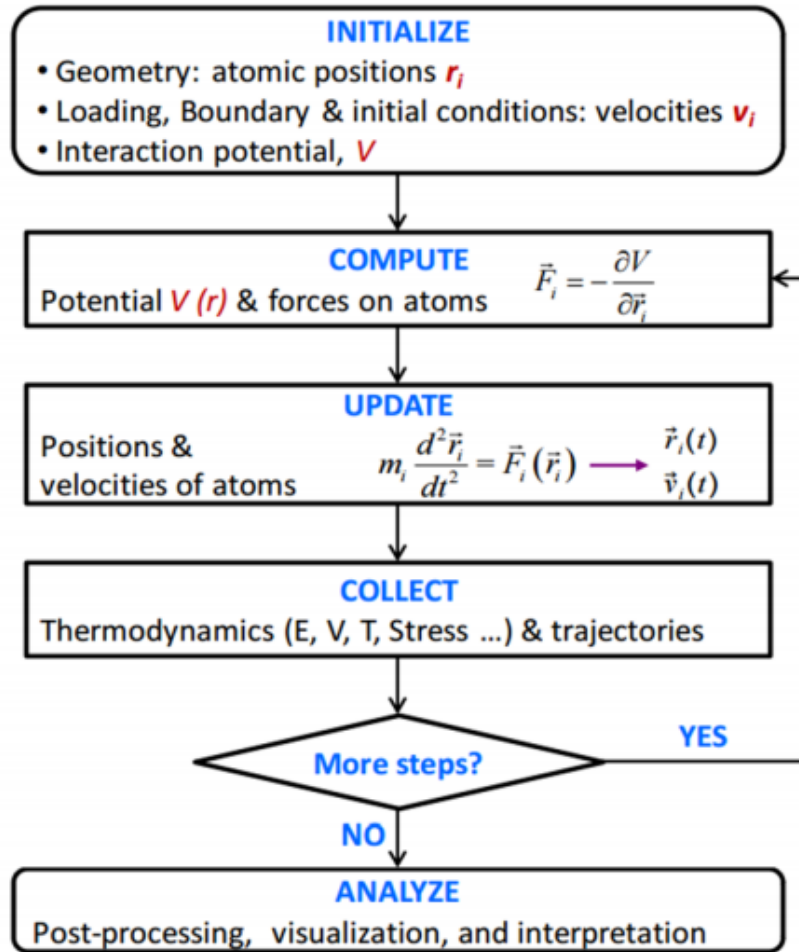


Figure 14: Flow chart of molecular dynamics simulation

3.8 Atomistic modeling of BNNTs

molecular dynamics is a widely used computational approach for simulation and characterization of the nanostructure because of their cost-effectiveness and less time consuming as compared to the experimental setup. MD forecast accurate interatomic interaction between molecules and atom and this is time-dependent behaviour of the system. this is done step by step by using the integration of newton's equation of motion[42]. MD simulation provides an edge over the continuum-based models and experiments with cost-efficient simulations. The fundamental advantage of

MD simulation over classical models is that it delivers a path dynamical property of the system such as transport coefficients, responses to perturbations, mechanical, and thermal properties, etc. [51], [52]. Therefore, MD simulation was performed in our work to investigate the buckling behaviour and piezoelectric response of defected and without defected BNNTs. In the present study, LAMMPS[53] simulator was used to perform all simulations. The Tersoff potential force field has been successfully used to study the piezoelectric and buckling behavior of BNNTs [45], [54], [55]. The Tersoff potential force field [56] was used to describe the potential field coefficient of interatomic interaction between boron-boron, nitrogen-nitrogen, and boron-nitrogen atoms of BNNTs for the present MD simulation. This potential energy is expressed as follows:

$$E = \frac{1}{2} \sum_i \sum_{j \neq i} V_{ij} \quad (11)$$

$$V_{ij} = f_c(r_{ij}) [f_R(r_{ij}) + b_{ij} f_A(r_{ij})] \quad (12)$$

$$f_c(r) = \begin{cases} 1 & : r < R - D \\ \frac{1}{2} - \frac{1}{2} \sin\left(\frac{\pi r - R}{2D}\right) & : R - D < r < R + D \\ 0 & : r > R + D \end{cases} \quad (13)$$

$$f_R(r) = A e^{-\lambda_1 r} \quad (14)$$

$$f_A(r) = -B e^{-\lambda_2 r} \quad (15)$$

Where,

V_{ij} = Bond energy

E = Energy of the system

r_{ij} = distance between atom i and j

b_{ij} = bond angle between atom I and j

$f_c(r)$ = cut-off function

$f_R(r_{ij})$ = repulsive pair potential

$f_A(r_{ij}) =$ attractive pair potential

The axial virial stress (σ) was averaged over time and position of all atoms, as follows[57]:

$$\sigma = \frac{1}{N} \sum_{i=1}^N \frac{1}{V_i} \left(m_i v_z^i v_z^i + \frac{1}{2} \sum_{j \neq i}^N F_z^{ij} r_z^{ij} \right) \quad (16)$$

where V_i is the volume of a tube, N is the number of atoms in a tube, F_z^{ij} is the interatomic potential force between the atoms i and j , r_i and r_j are the position vectors, r_z^{ij} is the interatomic distance in the axial direction between the i and j atoms, and m_i and v_z^i are the mass and velocity of atom i , respectively.

The investigation of the buckling behaviour of BNNTs under the influence of the electric field was accomplished by assuming the structure of BNNTs is a hollow continue cylinder with a wall thickness of 3.4 Å[58]–[60]. The cross-sectional area of BNNTs is given as,

$$A = \frac{\pi}{4} (D_o^2 - D_i^2) \quad (17)$$

and volume (V),

$$V = Al \quad (18)$$

where A is a cross-sectional area, D_i is inner diameter and D_o is outer diameter, the thickness of BNNTs is t , the volume is represented as V , the length is l and the Aspect ratio (L/D) was considered as 15[45]. The engineering strain is calculated by,

$$\varepsilon = \frac{\Delta l}{l_0} \quad (19)$$

where l_0 is the original length of nanosheet after minimization. Strain ε and electric field E_3 is applied along the axial direction of BNNTs and force of $f_i = q_i E_3$ is generated, where q_i charge of ion I ($+2.6e$ for $B^{2.6+}$ and $-2.6e$ for $N^{2.6-}$), is generated in BNNTs[34]. To applied E-field on BNNTs

The molecular dynamics simulation was performed in the following manner: First, the initial structure of BNNTs was prepared. Then relaxed the initial configuration (50 ps was used) by using a conjugate gradient method to minimize their energy from residual stresses. to reach the equilibrium stage it is considered that if the potential energy of the system is less than 1.0×10^{-10} kcal/mol. Here we use constant volume and temperature ensemble (NVT) and take time step as 0.5 fs and total time is 50 ps for reach equilibrium in BNNTs nanostructure. further classical equation of motion is integrate using the velocity verlet algorithm[61].

The defects occurred in BNNTs when it goes manufacturing process these defects change properties of the nanostructure. here we consider two types of defects stone-wales defect and vacancy defect. vacancy defect occurs randomly in nanostructure there for we generate random vacancy defect concentration. this concentration of vacancy defects affects the properties of BNNTs. The figure shows the vacancy defect concentration. following relation is used to calculate the vacancy defect concentration (ρ),

$$\rho = \frac{N_v}{N} \times 100\% \quad (20)$$

where

N_v = number of atom removed,

N = Total number of atoms present in BNNT.

To create a vacancy defect, boron and nitrogen atoms are removed as shown in figure 15, At present study considered: $\rho=0\%$ (pristine), 1%, 2%, 3% and 4% vacancy concentrations.

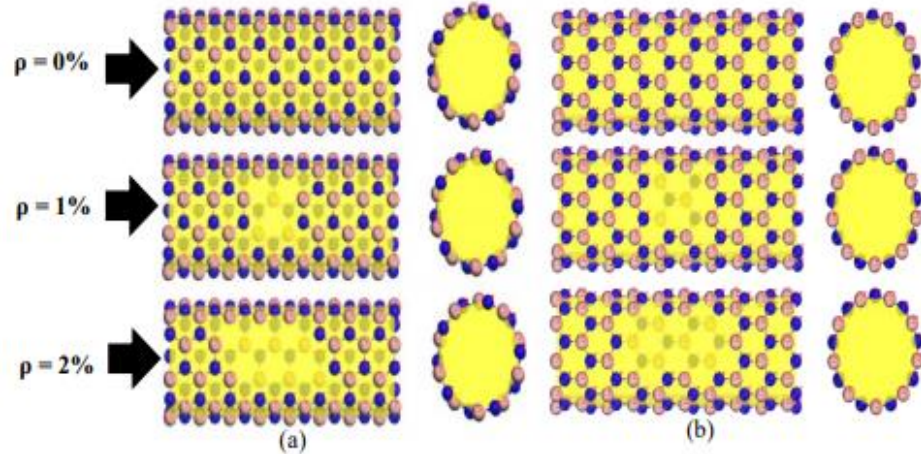


Figure 15: Different concentration vacancy defect

A stone-wales defect is a defect in which connectivity of two π -bond is changed and this π -bond rotates 90° with respect to their midpoint of their bond. And converting the four adjacent six-member rings into two pentagon/heptagon pairs. The stone-Wales defects are calculating the number of π -bond here we consider 0 (pristine), 1, 2, and 4 stone-Wales defects.

The piezoelectric constant is calculated using Maxwell equations [62], [63] which is the negative slope of stress and electric field curve and given as:

$$e_{33} = -\frac{\partial \sigma}{\partial E_3} \quad (21)$$

Where e_{33} is piezoelectric constant is compressive stress and E_3 is the electric field along the length.

To investigate the effect of different chirality on piezoelectric constant. The selection of different chiral BNNTs was based on the fact that they have maintained L/D ratio as 15 and length constant. One type of (10, 10) armchair BNNTs were considered.

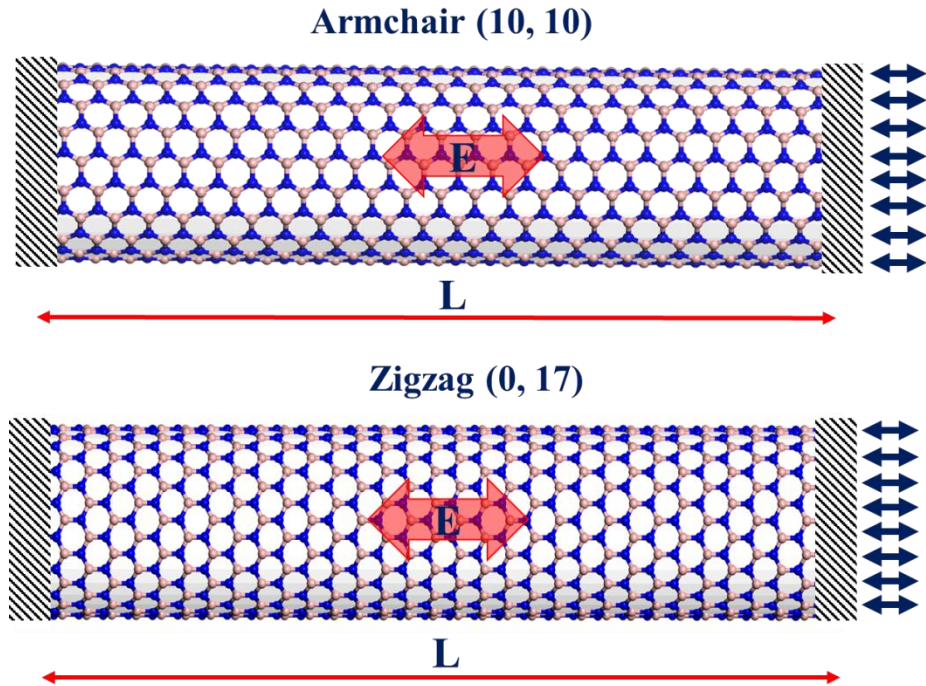


Figure 16: Schematic representation of applied electric field on (a) armchair and (b) zigzag BNNTs

3.9 Genetic programming model

Genetic programming used for the symbolic regression problem. In our study, we use molecular dynamics simulation data for forming a relationship between length and vacancy effect with the output variable piezoelectric coefficient.

The first initial population is generated by taking randomly element from the function and terminal sets. This element is a mathematical operator in the present work we are using two types of elements first one is arithmetic operators (+, -, ÷, ×), and the second one is non-linear elements like (sin, cos, tan, exp, tanh, log). The elements of the terminal set are input process variables and random constants. In our work, we use two input process variable length and vacancy defect concentration. Fitness function is used to see the performance on the input variable, this fitness function is

compared of actual values and predicted values of the GP model. the fitness function value minimum for getting better results. therefor we use root mean square error (RMSE) is given by

$$RMSE = \sqrt{\frac{\sum_{i=1}^N |G_i - A_i|^2}{N}} \quad (22)$$

where G_i is the predicted value for the i th data sample by the genetic programming model, A_i is the actual value of the i th data sample, and N is the number of training samples.

initial population performance is checked using termination criteria, this termination criteria is defined by the user and this is the threshold error of the model. if the initial population not performing according to us then a new population is generated by performing some genetic operations like mutation, crossover. for the genetic operations, tournament selection method is used. and genetic diversity is maintained by this. The crossover operation, namely, subtree crossover is used. Figure 17 shows the functioning of a subtree crossover in which the branch of the two models is chosen randomly and swapped.

subtree crossover method is used in the genetic programming Figure shows the functioning of a subtree crossover. in this randomly two branches select and exchange with each other. the randomly generated subtree is replaced by the branch of the model and this is called subtree mutation. in the present model reproduction probability rate is taken as 10%, the mutation probability rate is 5%, and the crossover probability rate is 85%. this shows that a large number of the population comes from crossover operation in the GP model. this whole process runs upto which termination criteria reaches and selection of the best model is done using minimum RMSE and this is performed using test data.

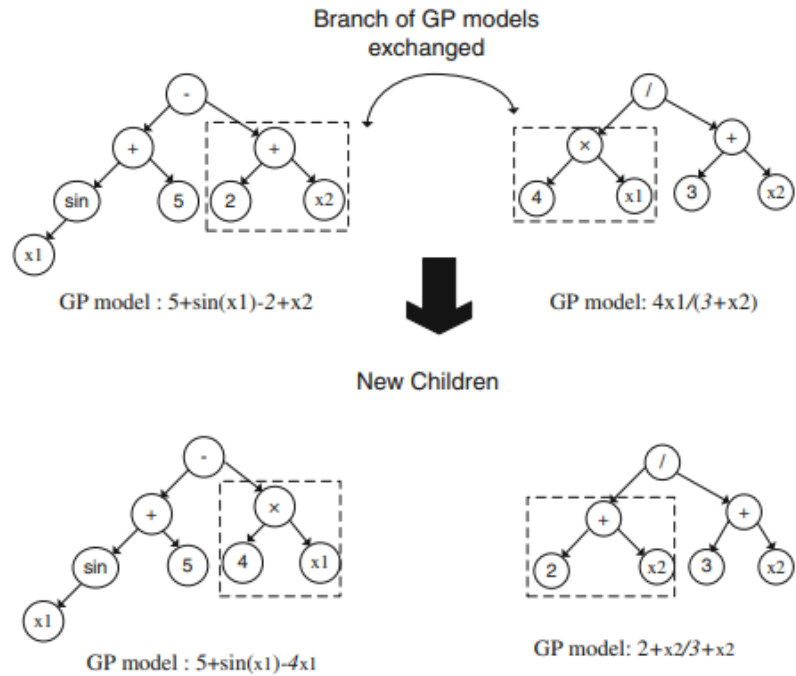


Figure 17: Subtree crossover operation

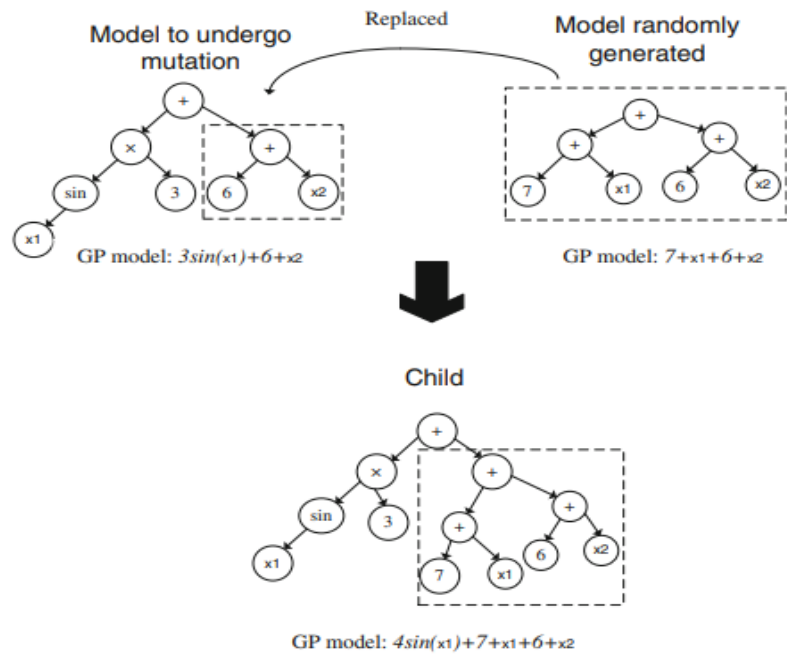


Figure 18: Subtree mutation operation

Chapter 4 Results and discussion

To effect of the electric field (E_1) on vacancies and stone wales defects were considered to determine the axial piezoelectric coefficient of both armchair (10, 10) and zigzag (0, 17)BNNTs.First, the MDS was performed on the pristine BNNTs subjected to the electric field E_1 from -0.25kV/cm to 0.25kV/cm. Figure 19 shows the relationship between axial compressive stress-axial compressive strain relationship curve. In the present From Figure 19 the compressive axial strain and axial stresswere considered as positive. The stress-strain curve of zigzag BNNTs without the effects of E_1 was tasted at the different stages as shown in Figure. 20. Which were associated with points A,B, C on the positive compressive stress-strain curve.Figure 20 shows stage A in which nanotube is inarelaxed position, and buckling starts. at point B it reaches its critical point this is the failure point of nanotube and stress associated with this point is called critical stress and at point B strain value is called critical buckling strain. as increasing strain after a point, B leads to a decrease in stress drastically.The position is called stable equilibrium if critical strain value is larger then axial average strain. if critical strain value is smaller than axial strain then BNNTs are in an unstable position.Different steps of buckling deformation of BNNTs are shown in Figure 20.

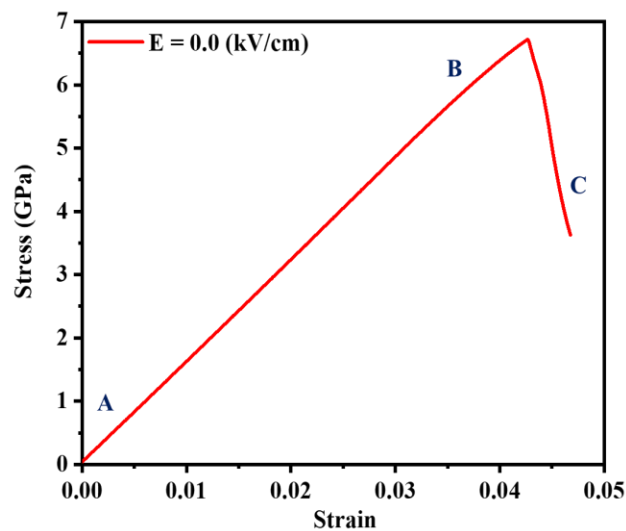


Figure 19: Axial compressive stress-strain curve for BNNTs

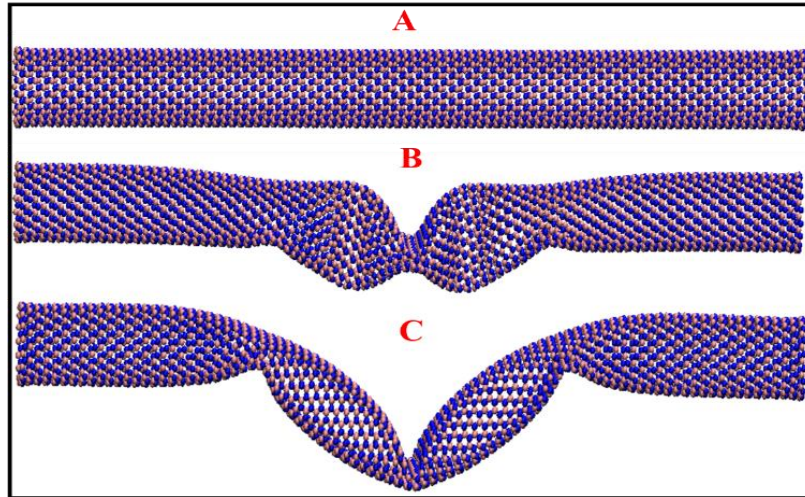


Figure 20: Structures of BNNTs under compression from points A to C.

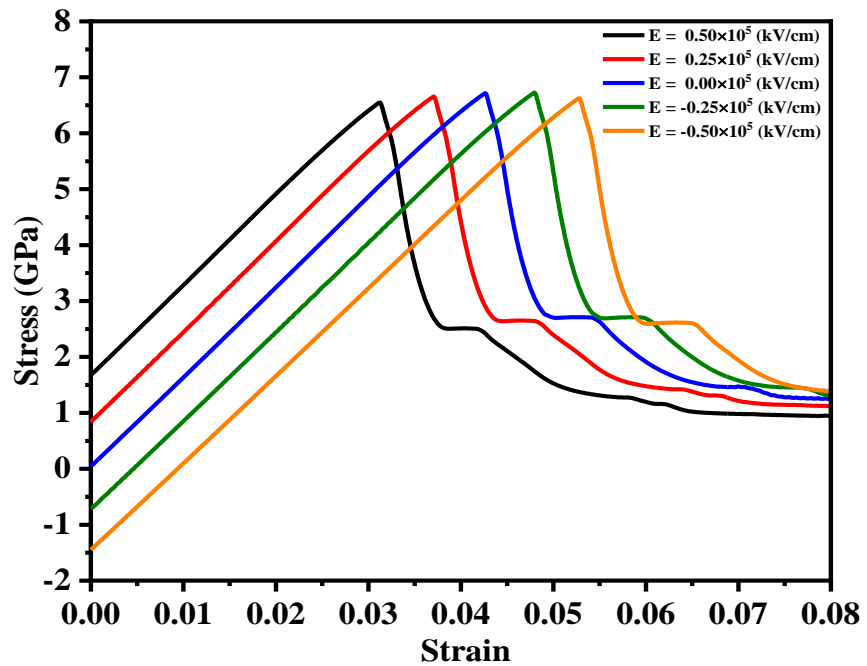


Figure 21: Stress-strain curve of zigzag (0, 17) BNNTs subjected to the different electric field.

The axial compressive stress and strain relationship for zigzag (0, 17) and armchair (10, 10) with different E_1 are plotted in Figures 21 and 22. As shown from Figure 21 (zigzag BNNTs) that the applied E_1 increases form

-0.5×10^5 kV/cm - 0.5×10^5 kV/cm and the critical buckling stress for different E_1 was found to be constant that is around 6.7 GPa with variation less than $\pm 1\%$. the reduction of critical buckling strain occurs almost 68% in this process as shown in Figure 21. the reason for piezoelectricity in BNNTs is because B and N atom are distributed along with the tube axis layer by layer which causes spontaneous polarization and produces piezoelectricity properties [44], [79].

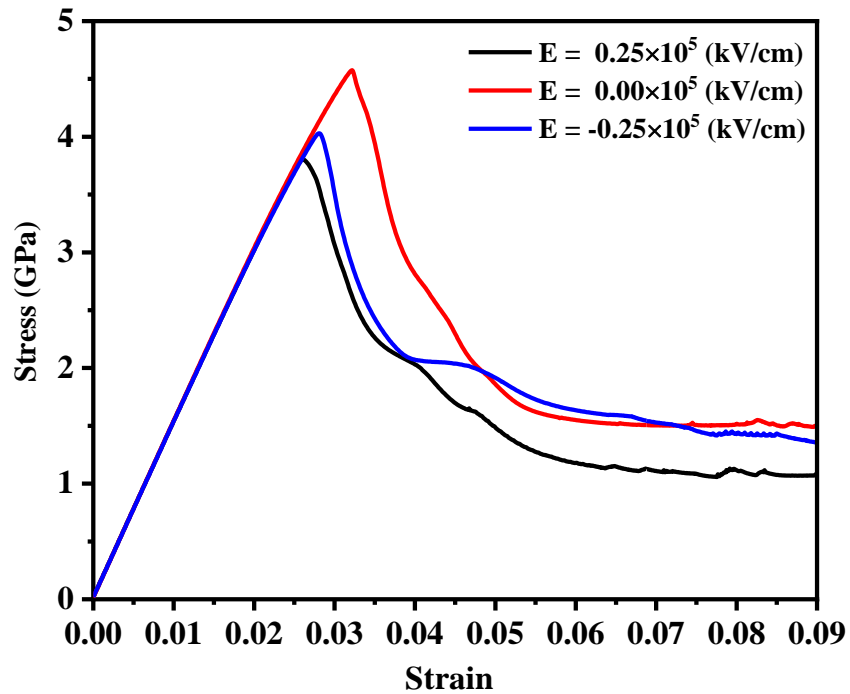


Figure 22: Stress-strain curve of Armchair (10, 10) BNNTs subjected to the different electric field

Similarly, as seen from Figure 22 that the armchair (10, 10) BNNTs, the applied E_1 increases from -0.25×10^5 kV/cm to 0.25×10^5 kV/cm the critical buckling stress was identified around 4.1 GPa with a variation of $\pm 9\%$ at the critical buckling strain 0.032 with a variation of $\pm 7\%$ this occurs due to their unit cell structure of BNNTs [64] before reached the buckling stage at axial compressive stress and strain is almost same for all three E_1 this was identified in armchair BNNTs because along the tube axis at each layer B and N are in same numbers, Therefore it will

not show any effect due to change in the E_1 and also, this is cause null value of spontaneous polarization, therefore, no piezoelectricity found.

In the previous sets of results, it was identified that only zigzag BNNTs shows the piezoelectric effect and piezoelectric effect was not to be identified from armchair BNNTs. Therefore, the piezoelectric effect of zigzag (0, 17) BNNTs were considered to determine the axial compressive stress vs E_1 curve as shown in Figure. 23. It can be observed from Figure. 6 that compressive stress and E_1 follow the linear relationship due to the converse piezoelectric effect. The piezoelectric coefficient was calculated using the Maxwell relation, and it was equal to the negative slope of the stress- electric field E_1 curve. The current predictions of piezoelectric coefficients of zigzag BNNTs were found to be 0.32 C/m^2 .

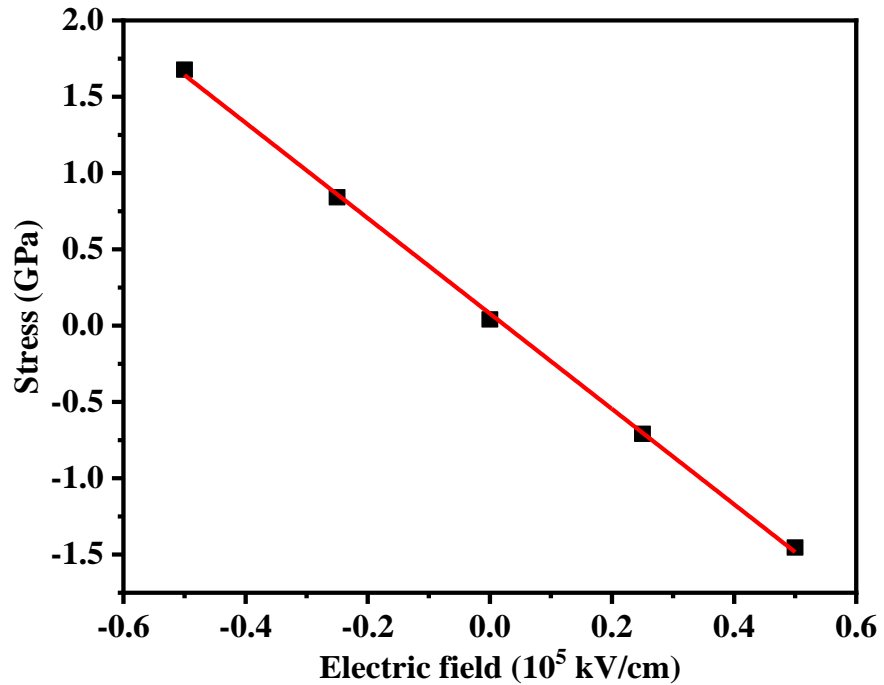


Figure 23: Variation of stresses in pristine (0, 17) BNNTs with the Electric field.

4.1 Effect of vacancy defect

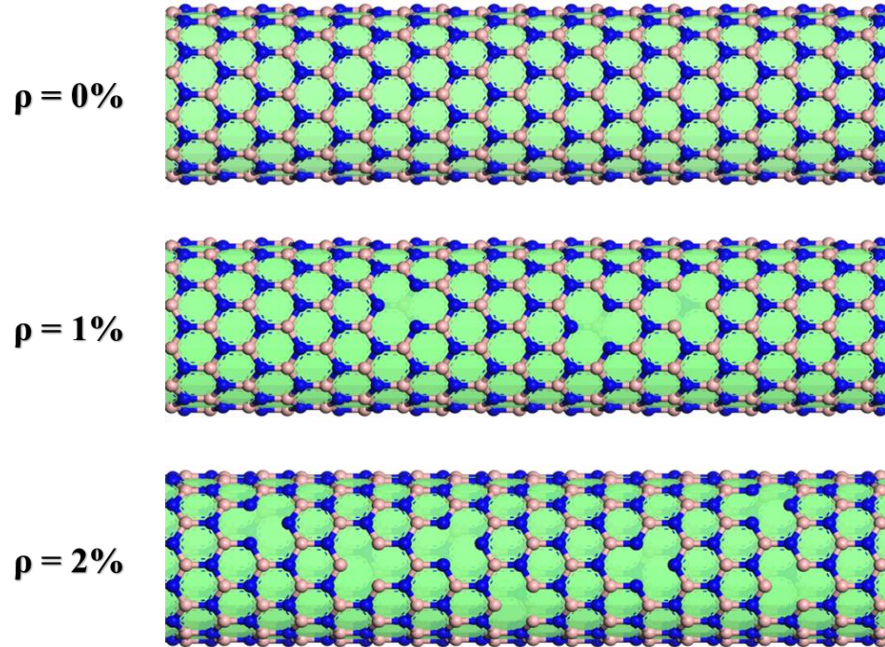


Figure 24: Schematic representation of vacancy concentration of 0%, 1% and 2% for zigzag (0, 17) BNNTs.

Table. 1 Buckling stress and buckling strain of different vacancy defected BNNTs.

| <i>Vacancy defect concentration</i> | 0% | 1% | 2% | 3% | 4% |
|--|-----------|-----------|-----------|-----------|-----------|
| <i>Buckling stress (GPa)</i> | 6.71 | 4.24 | 3.63 | 3.09 | 2.76 |
| <i>Buckling strain</i> | 0.042 | 0.031 | 0.030 | 0.029 | 0.028 |
| <i>Piezoelectric coefficient (C/m²)</i> | 0.31 | 0.28 | 0.25 | 0.23 | 0.21 |

Figure 25 shows the axial compressive stress-strain plot of vacancy defected zigzag (0, 17) BNNTs subjected to the different E_1 . The vacancy

defect was generated randomly and the concentration of vacancy was considered as percentages wise such as 0% (pristine), 1%, 2%, 3%, and 4% as shown in Figure. 25. For pristine BNNTs when strain reaches 0.042 the critical buckling stress obtain is 6.7 GPa. In the case of 1% vacancy, the buckling stress and strain were reduced up to 4.2 GPa and 0.031, almost 59%, and 35% reduction was identified in buckling stress and strain. All 4 cases are shown in Table 1. From Table 1 it was identified that as increases the concentration of vacancy defect buckling stress and strain value decreases linearly. The matter of fact was identified that the initial structure is maintaining the symmetrical structure for buckling and it will require more amount of energy as compared to defected BNNT. In the case of vacancy defected BNNTs, the boron nitrogen bond was broken an atom is absent from their position therefore it will not maintain symmetry and it will require less amount of energy to break the first bond and reach the buckling stage.

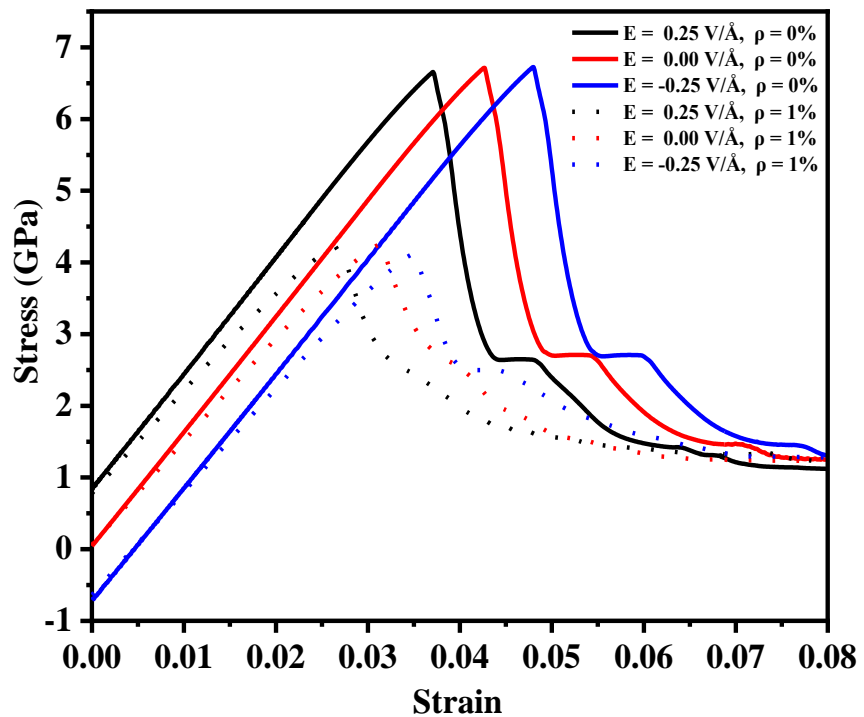


Figure 25: The stress-strain curve with vacancy defect zigzag BNNTs.

Among all other properties, the polarization of BNNTs was found to be very sensitive to vacancy defects, in the real case, due to the vacancy atom is absent from their location randomly. Therefore, further MD simulation was performed to investigate the effect of vacancies on the piezoelectric properties of BNNTs by creating vacancies in such a way that randomness is maintained. Figure 26 shows the stress-electric field curve of different vacancy concentrations of BNNTs. The piezoelectric coefficient is calculated by considering the negative slope of the stress-electric field curve and as vacancy concentration changes from 0% to 4%, the slope was decreased. Therefore, the value of the piezoelectric coefficient decreases from 0.31 C/m^2 to 0.21 C/m^2 .

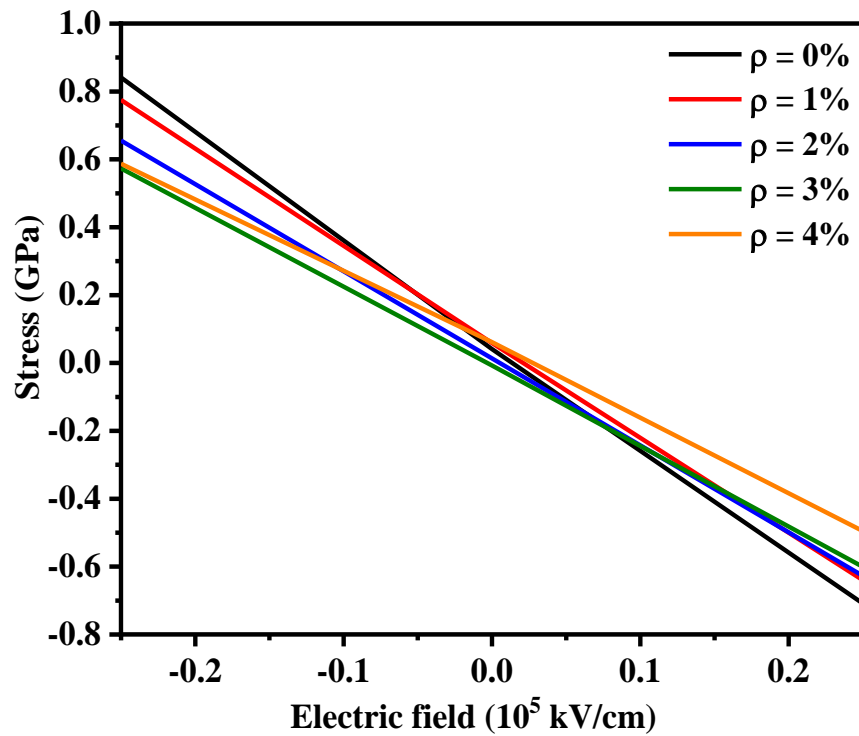


Figure 26: Stress-electric field curve vacancy defected zigzag BNNTs.

4.2 Stone-wales defect effect

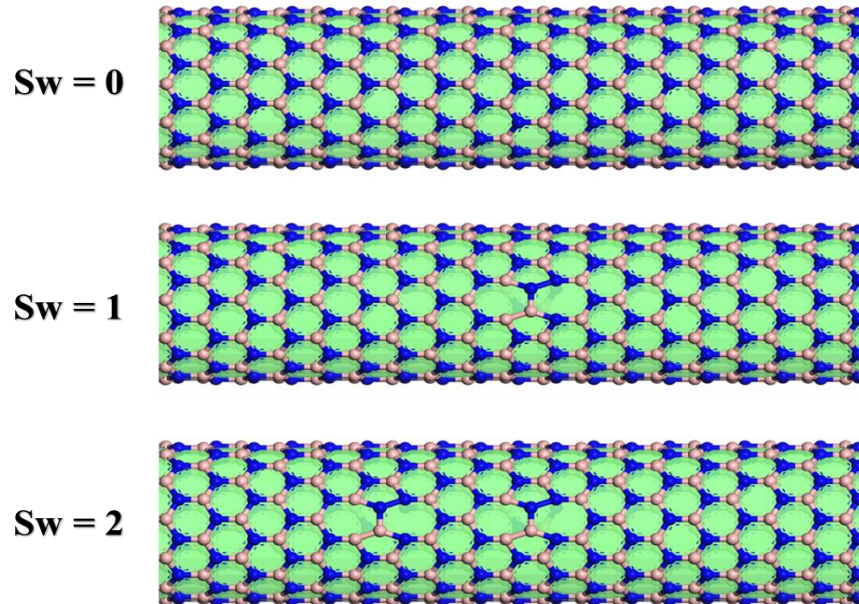


Figure 27: Schematic representation of stone wales defects by rotating B–N bonds 0, 1, and 2 for zigzag (0, 17) BNNTs.

Table.2 Buckling stress and buckling strain of different stone wales defected BNNTs

| <i>Stone-wales defect</i> | 0 | 1 | 2 | 4 |
|--|----------|----------|----------|----------|
| <i>Buckling stress (Gpa)</i> | 6.71 | 3.35 | 3.86 | 3.91 |
| <i>Buckling strain</i> | 0.042 | 0.022 | 0.025 | 0.026 |
| <i>Piezoelectric coefficient (C/m²)</i> | 0.312 | 0.308 | 0.308 | 0.306 |

The SW defect creates when a boron nitrogen bond considering in between two hexagons and this boron nitrogen bond rotates by 90⁰ about

an axis. After transformation, these B-N bonds converted into N-N and B-B bonds. Four hexagonal cells as shown in Figure. 1 atom then transform into two pair of heptagonal and pentagonal 7/5/5/7, respectively [65]. In the present study considered zigzag (0, 17) BNNT subjected to different electric field -2.5 to 2.5 kV/cm. The Schematic representation of stone wales defects considered as rotating 1, 2, and 4 boron nitrogen bonds as shown in Figure 28.

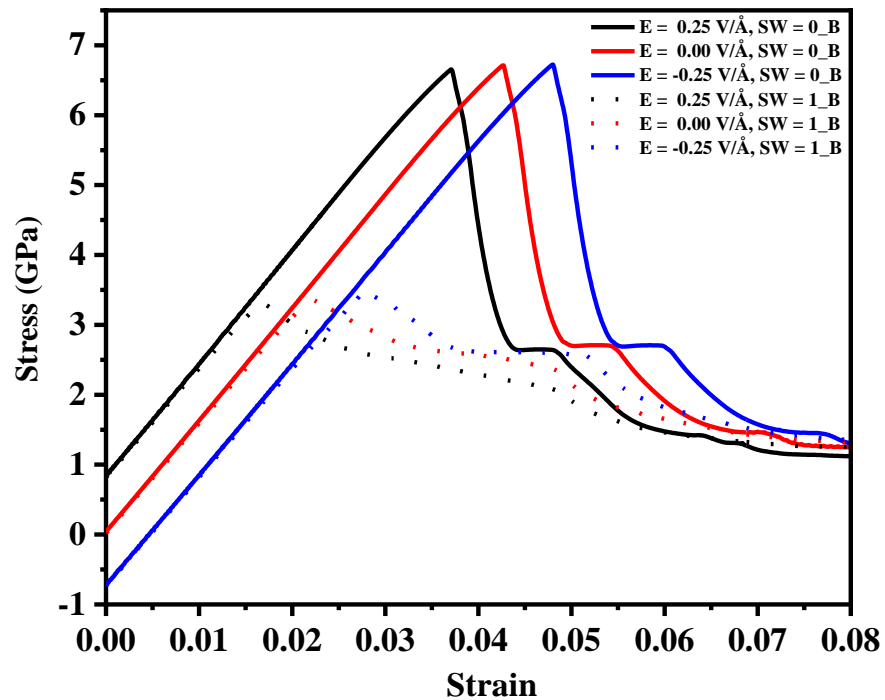


Figure 28: The stress-strain curve with stone-wales defect zigzag BNNTs.

Figure 28 shows the stress-strain plot of Stone-Wales defected zigzag (0, 17) BNNTs subjected to the different electric fields. The different stone-wales defect is creating by rotating B–N bonds 90^0 and by rotating 1, 2, and 4 number of B–N Bonds. For pristine at 0.042 strain value critical buckling stress is obtained is 6.7GPa in case of 1 stone-wales defect BNNTs buckling stress is reduced to 3.35 GPa and strain is reduced to 0.022 All 4 cases are shown in table 2, from table 2 we can see that as we increase stone-wales defect buckling stress value slightly increases also buckling strain value increases. This is happening because of the

change in their initial structure. And if we see the piezoelectric effect of BNNTs subjected to stone-wales, as we increase the stone-wales defect from 1 to 4 the piezoelectric coefficient is decreased but this change is very small. To see the variation in the buckling process step-by-step snapshots of the zigzag BNNT under uniaxial compression loadings are shown in Figure. 12, respectively

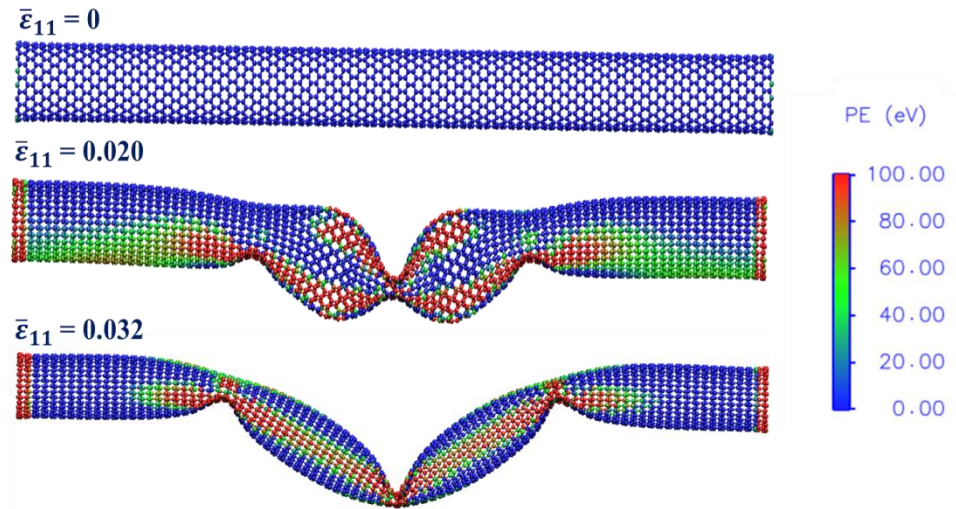


Figure 29: The snapshot of failure process in BNNTs under axial compression loading of zigzag (0, 17) BNNT.

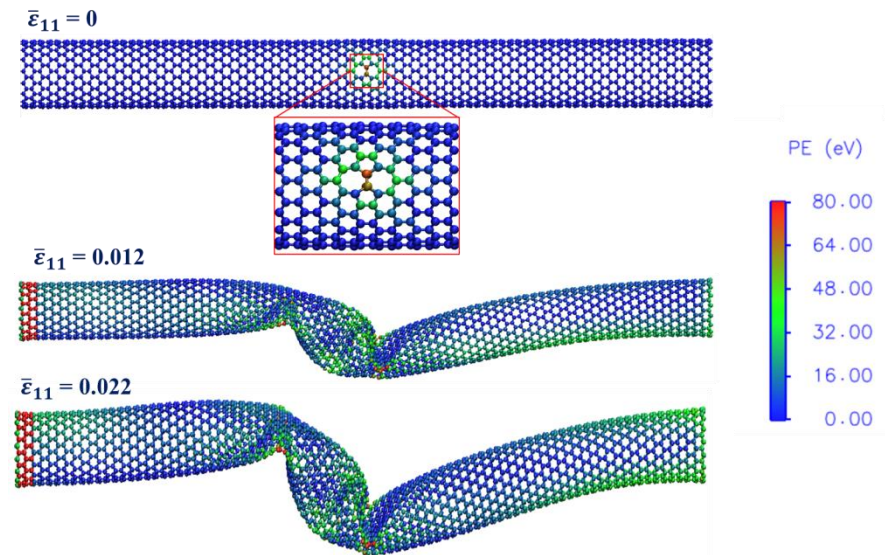


Figure 30: The snapshot of the failure process of stone wales defected BNNTs under axial compression loading of zigzag (0, 17) BNNT.

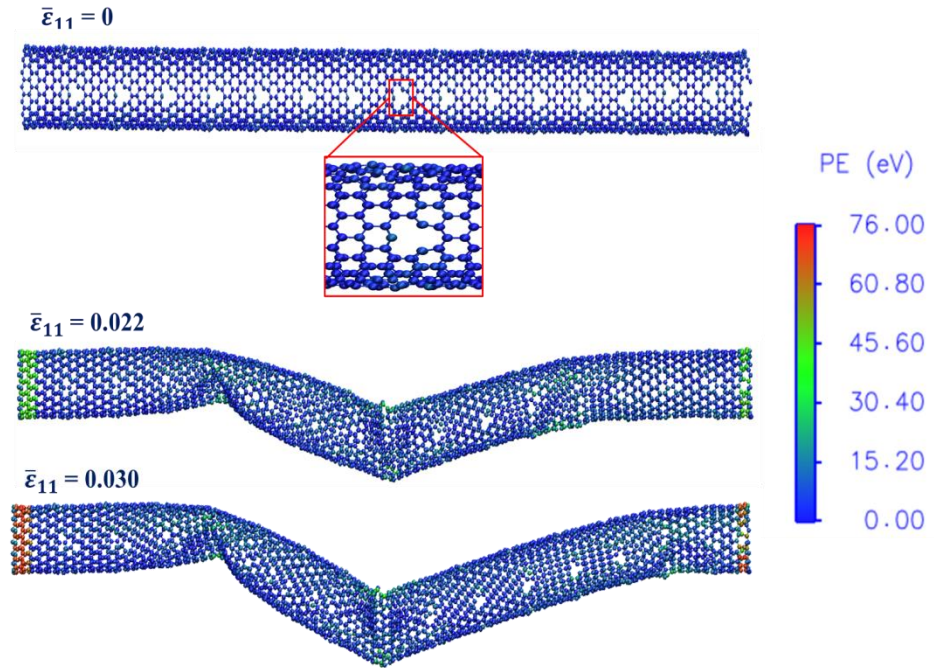


Figure 31: The snapshot of the failure process of vacancy defected BNNTs under axial compression loading of zigzag (0, 17) BNNT

4.3 Genetic programming

The data obtained from molecular dynamics simulation is used for the genetic programming method to formulate a relationship between the length of BNNTs (x_1) and a number of vacancy defects (x_2) and piezoelectric coefficient (y) is used as output variable all this data is obtained from MD simulation. learning of model is majorly dependent on how we select the training sample that's why 70% of randomly chosen data is used as a training sample and remaining data is used as testing samples. this data feed into cluster we created using an integrated computational model which is genetic programming model.

For creating the GP model we used python library Gplearn. this library is used for implementation, evaluation, and other processes for the selection of the piezoelectric coefficient of BNNTs. for getting the best result from the proposed model we use the trial and error method to adjust the setting parameter you can see in Table 3. for the diversity of our model we choose a wide range of mathematical elements. generation set and population size

are chosen according to the problem. the maximum number of genes and dept is chosen 6 and 8 respectively according to data we have for BNNTs. The final proposed mathematical model obtained from the genetic programming model is shown below.

$$y = \text{sub}(\text{sub}(\text{sub}(\text{add}(x_1, x_0), \text{mul}(\text{div}(\text{neg}(0.769), \text{neg}(x_1))), \text{div}(\text{add}(\text{log}(\text{abs}(-0.100)), x_0), \text{inv}(-0.519))))), \text{mul}(x_1, \text{max}(x_1, \text{log}(\text{div}(\text{max}(\text{abs}(\text{mul}(x_1, x_1)), \text{inv}(-0.519)), x_1))))), \text{div}(\text{neg}(0.776), \text{add}(x_1, \text{inv}(-0.519))))$$

where,

y = piezoelectric coefficient,

x_1 = length of BNNTs,

x_2 = vacancy defects concentration in BNNTs

Table 3: Descriptive statistics of the input and output process variables obtained from MD simulations for BNNTs

| Statistical parameter | Length (x_1) | Number of vacancy defects (x_2) | Piezoelectric constant (y) |
|------------------------------|----------------------------------|---|--|
| Mean | 181.666667 | 2.055556 | 0.227354 |
| Standard error | 3.547069 | 0.337931 | 0.008711 |
| Median | 180.000000 | 2.000000 | 0.224965 |
| Standard deviation | 15.048940 | 1.433721 | 0.036959 |
| Variance | 226.470588 | 2.055556 | 0.001366 |
| | Length (x_1) | Number of | Piezoelectric |

| | | | |
|-----------------|------------|--|---------------------|
| | | vacancy defects (x₂) | constant (y) |
| Kurtosis | -1.464024 | -1.269737 | 0.217362 |
| Skewness | -0.084141 | 0.026336 | 0.666206 |
| Minimum | 160.000000 | 0.000000 | 0.175106 |
| Maximum | 200.000000 | 4.000000 | 0.313098 |

Table 4: Parameter settings for proposed MD based AI model

| Parameters | Values assigned |
|--------------------------------------|--|
| Population size | 100 |
| Number of generations | 100 |
| Tournament size | 3 |
| Max depth of tree | 6 |
| Max genes | 8 |
| Functional set (F) | ('add', 'sub', 'mul', 'div', 'sqrt', 'log', 'abs', 'neg', 'inv', 'max', 'min') |
| Terminal set (T) | (x ₁ , x ₂ , [-1 1]) |
| Crossover probability rate | 0.85 |
| Reproduction probability rate | 0.10 |
| Mutation probability rate | 0.05 |

4.4 Conclusion:

As the first of its kind, we report the piezoelectric coefficient and buckling analysis of BNNTs subjected to the electric field. Three-body Tersoff potential force field is used in molecular dynamics simulation for investigating the effect of stone-wales defect and vacancy defect in BNNTs also find the mathematical relationship between length and vacancy defect with output variable piezoelectric coefficient, our results match with the present study. Below is the summary of the results:

- The buckling strain strongly related to the electric field. when the electric field increases the buckling strain decreases for zigzag BNNTs. and for armchair BNNTs, there is no significant effect of the electric field in buckling strain.
- The change critical buckling stress is very less for armchair BNNTs and almost negligible for zigzag BNNTs.
- The buckling stress and piezoelectric coefficient is decreasing as we increase the concentration of vacancy defect. because of here change in structure.
- The buckling stress for the stone-wales defected BNNTs decreases on the other hand very small change in the piezoelectric coefficient.
- The mathematical model obtained from genetic programming shows the good result with an R-square value of 0.99 which is very good results.

Reference

- [1] R. Feynman, "There's plenty of room at the bottom," in *Feynman and Computation*, 2018.
- [2] D. C. Rapaport, R. L. Blumberg, S. R. McKay, and W. Christian, "The Art of Molecular Dynamics Simulation," *Comput. Phys.*, 1996, doi: 10.1063/1.4822471.
- [3] A. Szabo and N. Ostlund, "Modern quantum chemistry : introduction to advanced electronic structure theory / Attila Szabo, Neil S. Ostlund," *SERBIULA (sistema Librum 2.0)*. 2018.
- [4] A. Rubio, J. L. Corkill, and M. L. Cohen, "Theory of graphitic boron nitride nanotubes," *Phys. Rev. B*, 1994, doi: 10.1103/PhysRevB.49.5081.
- [5] J. Wu, B. Wang, Y. Wei, R. Yang, and M. Dresselhaus, "Mechanics and mechanically tunable band gap in single-layer hexagonal boron-nitride," *Mater. Res. Lett.*, 2013, doi: 10.1080/21663831.2013.824516.
- [6] E. Zapata-Solvas, D. Gómez-García, and A. Domínguez-Rodríguez, "Towards physical properties tailoring of carbon nanotubes-reinforced ceramic matrix composites," *Journal of the European Ceramic Society*. 2012, doi: 10.1016/j.jeurceramsoc.2012.04.018.
- [7] L. H. Li, J. Cervenka, K. Watanabe, T. Taniguchi, and Y. Chen, "Strong oxidation resistance of atomically thin boron nitride nanosheets," *ACS Nano*, 2014, doi: 10.1021/nn500059s.
- [8] J. X. Zhao and Y. H. Ding, "The effects of O₂ and H₂O adsorbates on field-emission properties of an (8, 0) boron nitride nanotube: A density functional theory study," *Nanotechnology*, 2009, doi: 10.1088/0957-4484/20/8/085704.
- [9] C. Tang, Y. Bando, X. Ding, S. Qi, and D. Golberg, "Catalyzed collapse and enhanced hydrogen storage of BN nanotubes," *J. Am. Chem. Soc.*, 2002, doi: 10.1021/ja028051e.
- [10] R. Ansari and S. Ajori, "Molecular dynamics study of the torsional vibration characteristics of boron-nitride nanotubes," *Phys. Lett. Sect. A Gen. At. Solid State Phys.*, 2014, doi: 10.1016/j.physleta.2014.08.006.
- [11] N. G. Chopra and A. Zettl, "Measurement of the elastic modulus of a multi-wall boron nitride nanotube," *Solid State Commun.*, 1998, doi: 10.1016/S0038-1098(97)10125-9.
- [12] M. R. Davoudabadi and S. D. Farahani, "Investigation of vacancy

defects on the young's modulus of carbon nanotube reinforced composites in axial direction via a multiscale modeling approach," *J. Solid Mech.*, 2010.

- [13] M. N. Nahas and M. Abd-Rabou, "Finite element modeling of carbon nanotubes," *Int. J. Mech. Mech. Eng.*, 2010.
- [14] C. J. Wu, C. Y. Chou, C. N. Han, and K. N. Chiang, "Simulation and validation of CNT mechanical properties - The future interconnection material," in *Proceedings - Electronic Components and Technology Conference*, 2007, doi: 10.1109/ECTC.2007.373835.
- [15] T. M. Schmidt, R. J. Baierle, P. Piquini, and A. Fazzio, "Theoretical study of native defects in BN nanotubes," *Phys. Rev. B*, vol. 67, no. 11, p. 113407, 2003, doi: 10.1103/PhysRevB.67.113407.
- [16] S. I. Kundalwal and V. Choyal, "Transversely isotropic elastic properties of carbon nanotubes containing vacancy defects using MD," *Acta Mech.*, 2018, doi: 10.1007/s00707-018-2123-5.
- [17] J. Song, H. Jiang, J. Wu, Y. Huang, and K. C. Hwang, "Stone-Wales transformation in boron nitride nanotubes," *Scr. Mater.*, 2007, doi: 10.1016/j.scriptamat.2007.06.027.
- [18] R. Ansari, M. Mirnezhad, and S. Sahmani, "Prediction of chirality- and size-dependent elastic properties of single-walled boron nitride nanotubes based on an accurate molecular mechanics model," *Superlattices Microstruct.*, 2015, doi: 10.1016/j.spmi.2014.12.033.
- [19] J. Wang, C. H. Lee, and Y. K. Yap, "Recent advancements in boron nitride nanotubes," *Nanoscale*. 2010, doi: 10.1039/c0nr00335b.
- [20] R. S. Ruoff and D. C. Lorents, "Mechanical and thermal properties of carbon nanotubes," *Carbon N. Y.*, 1995, doi: 10.1016/0008-6223(95)00021-5.
- [21] A. Rochefort, P. Avouris, F. Lesage, and D. R. Salahub, "Electrical and mechanical properties of distorted carbon nanotubes," *Phys. Rev. B - Condens. Matter Mater. Phys.*, 1999, doi: 10.1103/PhysRevB.60.13824.
- [22] R. Kothari, S. I. Kundalwal, and S. K. Sahu, "Transversely isotropic thermal properties of carbon nanotubes containing vacancies," *Acta Mech.*, 2018, doi: 10.1007/s00707-018-2145-z.
- [23] R. S. Ruoff, D. Qian, and W. K. Liu, "Mechanical properties of carbon nanotubes: Theoretical predictions and experimental measurements," *Comptes Rendus Physique*. 2003, doi:

10.1016/j.crhy.2003.08.001.

- [24] V. Choyal and S. I. Kundalwal, "Transversely isotropic elastic properties of carbon nanotubes containing vacancy defects using MD," *Acta Mech.*, pp. 1–22, 2018, doi: 10.1007/s00707-018-2123-5.
- [25] L. Shen and J. Li, "Transversely isotropic elastic properties of single-walled carbon nanotubes," *Phys. Rev. B - Condens. Matter Mater. Phys.*, 2004, doi: 10.1103/PhysRevB.69.045414.
- [26] K. M. Liew, C. H. Wong, X. Q. He, M. J. Tan, and S. A. Meguid, "Nanomechanics of single and multiwalled carbon nanotubes," *Phys. Rev. B - Condens. Matter Mater. Phys.*, 2004, doi: 10.1103/PhysRevB.69.115429.
- [27] Z. Kang, M. Li, and Q. Tang, "Buckling behavior of carbon nanotube-based intramolecular junctions under compression: Molecular dynamics simulation and finite element analysis," *Comput. Mater. Sci.*, 2010, doi: 10.1016/j.commatsci.2010.08.011.
- [28] Y. Yan, W. Q. Wang, and L. X. Zhang, "Nonlocal effect on axially compressed buckling of triple-walled carbon nanotubes under temperature field," *Appl. Math. Model.*, 2010, doi: 10.1016/j.apm.2010.02.031.
- [29] K. M. Liew and J. Yuan, "High-temperature thermal stability and axial compressive properties of a coaxial carbon nanotube inside a boron nitride nanotube," *Nanotechnology*, 2011, doi: 10.1088/0957-4484/22/8/085701.
- [30] A. Shokuhfar, S. Ebrahimi-Nejad, A. Hosseini-Sadegh, and A. Zare-Shahabadi, "The effect of temperature on the compressive buckling of boron nitride nanotubes," *Phys. Status Solidi Appl. Mater. Sci.*, 2012, doi: 10.1002/pssa.201127678.
- [31] S. Ebrahimi-Nejad and A. Shokuhfar, "Compressive buckling of open-ended boron nitride nanotubes in hydrogen storage applications," *Phys. E Low-Dimensional Syst. Nanostructures*, 2013, doi: 10.1016/j.physe.2013.02.021.
- [32] A. Salehi-Khojin and N. Jalili, "Buckling of boron nitride nanotube reinforced piezoelectric polymeric composites subject to combined electro-thermo-mechanical loadings," *Compos. Sci. Technol.*, 2008, doi: 10.1016/j.compscitech.2007.10.024.
- [33] A. Jafari, A. A. Khatibi, and M. Mosavi Mashadi, "Evaluation of mechanical and piezoelectric properties of boron nitride nanotube: A novel electrostructural analogy approach," *J. Comput. Theor.*

Nanosci., 2012, doi: 10.1166/jctn.2012.2047.

- [34] J. Zhang, C. Wang, and S. Adhikari, "Fracture and buckling of piezoelectric nanowires subject to an electric field," *J. Appl. Phys.*, 2013, doi: 10.1063/1.4829277.
- [35] V. Yamakov, C. Park, J. H. Kang, K. E. Wise, and C. Fay, "Piezoelectric molecular dynamics model for boron nitride nanotubes," *Comput. Mater. Sci.*, 2014, doi: 10.1016/j.commatsci.2014.07.047.
- [36] V. Yamakov, C. Park, J. H. Kang, X. Chen, C. Ke, and C. Fay, "Piezoelectric and elastic properties of multiwall boron-nitride nanotubes and their fibers: A molecular dynamics study," *Comput. Mater. Sci.*, 2017, doi: 10.1016/j.commatsci.2017.03.050.
- [37] S. M. Nakhmanson, A. Calzolari, V. Meunier, J. Bernholc, and M. B. Nardelli, "Spontaneous polarization and piezoelectricity in boron nitride nanotubes," *Phys. Rev. B - Condens. Matter Mater. Phys.*, 2003, doi: 10.1103/PhysRevB.67.235406.
- [38] J. Zhang, "Elastocaloric effect on the piezoelectric potential of boron nitride nanotubes," *J. Phys. D. Appl. Phys.*, 2017, doi: 10.1088/1361-6463/aa839e.
- [39] Y. Zhang, Y. Bai, and B. Yan, "Functionalized carbon nanotubes for potential medicinal applications," *Drug Discovery Today*. 2010, doi: 10.1016/j.drudis.2010.04.005.
- [40] N. G. Chopra *et al.*, "Boron nitride nanotubes," *Science (80-.)*, 1995, doi: 10.1126/science.269.5226.966.
- [41] Y. Li, Z. Zhou, D. Golberg, Y. Bando, P. R. Von Schleyer, and Z. Chen, "Stone-Wales defects in single-walled boron nitride nanotubes: Formation energies, electronic structures, and reactivity," *J. Phys. Chem. C*, 2008, doi: 10.1021/jp077115a.
- [42] M. Griebel, J. Hamaekers, and F. Heber, "A molecular dynamics study on the impact of defects and functionalization on the Young modulus of boron-nitride nanotubes," *Comput. Mater. Sci.*, 2009, doi: 10.1016/j.commatsci.2009.03.029.
- [43] E. N. C. Paura, W. F. Da Cunha, J. B. L. Martins, G. M. E Silva, L. F. Roncaratti, and R. Gargano, "Carbon dioxide adsorption on doped boron nitride nanotubes," *RSC Adv.*, 2014, doi: 10.1039/c4ra00432a.
- [44] H. Wang, N. Ding, X. Zhao, and C. M. L. Wu, "Defective boron nitride nanotubes: Mechanical properties, electronic structures and

failure behaviors,” *J. Phys. D. Appl. Phys.*, 2018, doi: 10.1088/1361-6463/aaabfa.

- [45] V. Choyal, V. K. Choyal, and S. I. Kundalwal, “Effect of atom vacancies on elastic and electronic properties of transversely isotropic boron nitride nanotubes: A comprehensive computational study,” *Comput. Mater. Sci.*, vol. 156, pp. 332–345, Jan. 2019, doi: 10.1016/J.COMMATSCI.2018.10.013.
- [46] H. Zeighampour and Y. Tadi Beni, “Buckling analysis of boron nitride nanotube with and without defect using molecular dynamic simulation,” *Mol. Simul.*, 2020, doi: 10.1080/08927022.2019.1697817.
- [47] Y. JUNG, “Introduction to a Molecular Dynamics Simulation,” *Phys. High Technol.*, 2012, doi: 10.3938/phit.21.037.
- [48] C. Y. Zhi, Y. Bando, T. Terao, C. C. Tang, H. Kuwahara, and D. Golberg, “Chemically activated boron nitride nanotubes,” *Chem. - An Asian J.*, 2009, doi: 10.1002/asia.200900158.
- [49] Y. Jin and F. G. Yuan, “Simulation of elastic properties of single-walled carbon nanotubes,” *Compos. Sci. Technol.*, 2003, doi: 10.1016/S0266-3538(03)00074-5.
- [50] H. Sun, “Ab Initio Calculations and Force Field Development for Computer Simulation of Polysilanes,” *Macromolecules*, 1995, doi: 10.1021/ma00107a006.
- [51] K. Matsunaga and Y. Iwamoto, “Molecular Dynamics Study of Atomic Structure and Diffusion Behavior in Amorphous Silicon Nitride Containing Boron,” *J. Am. Ceram. Soc.*, vol. 84, no. 10, pp. 2213–2219, 2004, doi: 10.1111/j.1151-2916.2001.tb00990.x.
- [52] B. Mortazavi and Y. Rémond, “Investigation of tensile response and thermal conductivity of boron-nitride nanosheets using molecular dynamics simulations,” *Phys. E Low-Dimensional Syst. Nanostructures*, vol. 44, no. 9, pp. 1846–1852, 2012, doi: 10.1016/j.physe.2012.05.007.
- [53] S. J. Plimpton, “Computational Limits of Classical Molecular Dynamics Simulations 1 Introduction 2 Parallel MD,” *LAMMPS, Sandia Natl. Lab.*, pp. 1–8, 1995.
- [54] N. M. Anoop Krishnan and D. Ghosh, “Chirality dependent elastic properties of single-walled boron nitride nanotubes under uniaxial and torsional loading,” *J. Appl. Phys.*, vol. 115, no. 6, 2014, doi: 10.1063/1.4864781.

- [55] V. Verma, V. K. Jindal, and K. Dharamvir, "Elastic moduli of a boron nitride nanotube," *Nanotechnology*, vol. 18, no. 43, 2007, doi: 10.1088/0957-4484/18/43/435711.
- [56] J. Tersoff, "New empirical approach for the structure and energy of covalent systems," *Phys. Rev. B*, vol. 37, no. 12, pp. 6991–7000, 1988, doi: 10.1103/PhysRevB.37.6991.
- [57] A. K. Subramaniyan and C. T. Sun, "Continuum interpretation of virial stress in molecular simulations," *Int. J. Solids Struct.*, 2008, doi: 10.1016/j.ijsolstr.2008.03.016.
- [58] K. N. Kudin, G. E. Scuseria, and B. I. Yakobson, "C₂F, BN, and C nanoshell elasticity from ab initio computations," *Phys. Rev. B - Condens. Matter Mater. Phys.*, 2001.
- [59] M. Santosh, P. K. Maiti, and A. K. Sood, "Elastic properties of Boron Nitride Nanotubes and their comparison with carbon Nanotubes," in *Journal of Nanoscience and Nanotechnology*, 2009, doi: 10.1166/jnn.2009.1197.
- [60] E. S. Oh, "Elastic properties of boron-nitride nanotubes through the continuum lattice approach," *Mater. Lett.*, 2010, doi: 10.1016/j.matlet.2010.01.041.
- [61] V. Choyal, V. K. Choyal, and S. I. Kundalwal, "Transversely isotropic elastic properties of vacancy defected boron nitride nanotubes using molecular dynamics simulations," in *2018 IEEE 13th Nanotechnology Materials and Devices Conference, NMDC 2018*, 2019, doi: 10.1109/NMDC.2018.8605862.
- [62] K. A. N. Duerloo, M. T. Ong, and E. J. Reed, "Intrinsic piezoelectricity in two-dimensional materials," *J. Phys. Chem. Lett.*, 2012, doi: 10.1021/jz3012436.
- [63] J. Zhang, C. Wang, and C. Bowen, "Piezoelectric effects and electromechanical theories at the nanoscale," *Nanoscale*. 2014, doi: 10.1039/c4nr03756a.
- [64] R. Ansari, M. Faghihnasiri, S. Malakpour, and S. Sahmani, "A DFT study on the elastic and structural properties of a (3,3) boron nitride nanotube under external electric field," *Superlattices Microstruct.*, 2015, doi: 10.1016/j.spmi.2015.01.036.
- [65] W. H. Moon and H. J. Hwang, "Molecular-dynamics simulation of structure and thermal behaviour of boron nitride nanotubes," *Nanotechnology*, vol. 15, no. 5, pp. 431–434, 2004, doi: 10.1088/0957-4484/15/5/005.